

1 This is a **preprint**

2 The article has been submitted for peer-review to the *Journal of Luminescence* as:

3 Riedesel, S., Duller, G.A.T., Ankjærgaard, C., submitted. Time-resolved infrared stimulated luminescence of the
4 blue and yellow-green emissions – insights into charge recombination in chemically and structurally different
5 alkali feldspars. *Journal of Luminescence*.
6

7

8 This is a **preprint**

9 The article has been submitted for peer-review to the *Journal of Luminescence* as:

10 Riedesel, S., Duller, G.A.T., Ankjærgaard, C., submitted. Time-resolved infrared stimulated
11 luminescence of the blue and yellow-green emissions – insights into charge recombination in
12 chemically and structurally different alkali feldspars. *Journal of Luminescence*.
13

14

15

16 **Time-resolved infrared stimulated luminescence of the blue and yellow-green emissions – insights
17 into charge recombination in chemically and structurally different alkali feldspars**
18

19

20 Svenja Riedesel^{1,2}, Geoff A.T. Duller², Christina Ankjærgaard³

21 ¹ Institute of Geography, University of Cologne, Albertus-Magnus-Platz, 50923 Köln/Cologne, Germany

22 ² Department of Geography and Earth Sciences, Aberystwyth University, Penglais Campus, Aberystwyth SY23 3DB, United
23 Kingdom

24 ³ Department of Health Technology, Technical University of Denmark, Risø Campus, 4000 Roskilde, Denmark
25
26
27
28

This is a **preprint**

The article has been submitted for peer-review to the *Journal of Luminescence* as:

Riedesel, S., Duller, G.A.T., Ankjærgaard, C., submitted. Time-resolved infrared stimulated luminescence of the blue and yellow-green emissions – insights into charge recombination in chemically and structurally different alkali feldspars. *Journal of Luminescence*.

19 **Time-resolved infrared stimulated luminescence of the blue and yellow-green emissions –**
20 **insights into charge recombination in chemically and structurally different alkali feldspars**

21

22 Svenja Riedesel^{1,2}, Geoff A.T. Duller², Christina Ankjærgaard³

23 ¹ Institute of Geography, University of Cologne, Albertus-Magnus-Platz, 50923 Köln/Cologne, Germany

24 ² Department of Geography and Earth Sciences, Aberystwyth University, Penglais Campus, Aberystwyth SY23 3DB, United
25 Kingdom

26 ³ Department of Health Technology, Technical University of Denmark, Risø Campus, 4000 Roskilde, Denmark

27 Corresponding author: Svenja Riedesel, riedeselsvenja@gmail.com

28

29 **Abstract**

30 Time-resolved luminescence measurements can be used to explore luminescence processes in
31 minerals and the defects involved. It has also been applied to feldspars and knowledge has been gained
32 regarding potential crystal defects associated with luminescence productions in these minerals, but
33 also regarding processes governing electron-hole recombination leading to luminescence emission.

34 Here we present time-resolved infrared stimulated luminescence (IRSL) signals measured for a range
35 of mineralogically well characterised single crystal alkali feldspars. We explore time-resolved
36 luminescence for the blue (~410 nm) and the yellow-green emission (~550 nm) in response to different
37 irradiation doses and by comparing different IRSL signals. Firstly, we explore whether the lifetimes
38 measured represent excited state or recombination lifetimes. Secondly, we investigate sample-
39 dependent changes in blue and yellow-green time-resolved signals and link those to physical
40 properties of the samples.

41 Our results show that the timescales on which the blue and the yellow-green emission occur differ
42 significantly, with the blue signal on the μs -scale, and the yellow-green emission on the ms-scale. We
43 do not observe any dependence of the time-resolved signal on signal integration, dose given or IRSL
44 signal measured. However, inter-sample variability is shown for both emissions. In the blue we only
45 observe small differences in decay time scale between single-phase feldspars and perthites, however
46 larger differences are measured between samples that were artificially disordered compared to
47 ordered feldspars. Longer lifetimes observed for disordered feldspars are suggested to be linked to
48 either changes in the recombination centre or to increased band-tail states transport due to an
49 increase in the width or density of the sub-conduction band-tail states. The data indicates the potential

This is a **preprint**

The article has been submitted for peer-review to the *Journal of Luminescence* as:

Riedesel, S., Duller, G.A.T., Ankjærgaard, C., submitted. Time-resolved infrared stimulated luminescence of the blue and yellow-green emissions – insights into charge recombination in chemically and structurally different alkali feldspars. *Journal of Luminescence*.

50 of using time-resolved IRSL of the blue emission to get an indication of the state of order of a feldspar.
51 For the yellow-green emission slow signal decays are observed for single-phase feldspars, likely
52 indicating a spin-forbidden transition. Interestingly, similar lifetimes were observed for K- and Na-
53 feldspar end members.

54 **Keywords**

55 Time-resolved luminescence, lifetime, feldspar, recombination, band-tail states

56 **1 Introduction**

57 Conventional luminescence measurements use continuous wave (CW) stimulation to excite trapped
58 electrons and enable their migration through the crystal lattice, resulting in recombination at a
59 recombination centre. If the recombination process is radiant it leads to the emission of photons. In
60 time-resolved (TR) luminescence measurements samples are stimulated using pulsed light, meaning
61 that a TR measurement consists of multiple stimulation light pulses, separated by so-called off-times,
62 during which no optical stimulation occurs (Sanderson and Clark, 1994; Lapp et al., 2009). This method
63 not only enables an improved discrimination of excitation and emission wavelengths, but also gives
64 information on recombination processes in minerals (Sanderson and Clark, 1994). During on-times of
65 pulsed stimulation, electrons are excited from the ground state of the electron trapping centres and
66 migrate to recombination centres, while the off-time allows investigations into the decay of different
67 luminescence emissions after the optical stimulation has been turned off. Thus, TR-luminescence
68 measurements make it possible to measure recombination lifetimes and excited state lifetimes of the
69 luminescence centres. For feldspars, TR-luminescence measurements have previously been performed
70 to gain insights into electron-hole recombination processes (e.g. Sanderson and Clark, 1994; Jain and
71 Ankjærgaard, 2011) and to understand defects involved in luminescence production and their
72 locations within the crystal lattice (e.g. Clark and Bailiff, 1998). Despite this previous research, it is still
73 unknown, how different chemistry and structure of feldspars impact luminescence production and
74 how these factors influence excited state and recombination lifetimes of feldspar infrared stimulated
75 luminescence (IRSL). In this paper we use TR-IRSL with detection in the blue (~410 nm) and yellow-
76 green (~550 nm) wavelength regions to explore recombination processes and potentially involved
77 defects in chemically and structurally different alkali feldspars.

78 Time-resolved luminescence with emissions in the UV, blue, yellow-green or red to near-infrared, have
79 been investigated, mainly to understand the defects and transitions involved in the recombination
80 process. The blue luminescence emission has been associated with a hole centre located on Al-O-Al

This is a **preprint**

The article has been submitted for peer-review to the *Journal of Luminescence* as:

Riedesel, S., Duller, G.A.T., Ankjærgaard, C., submitted. Time-resolved infrared stimulated luminescence of the blue and yellow-green emissions – insights into charge recombination in chemically and structurally different alkali feldspars. *Journal of Luminescence*.

81 bridges (Finch and Klein, 1999; Riedesel et al., 2021a) and it has been shown that its intensity and
82 stability is dependent on the degree of order on the Si, Al-framework and on the presence and type of
83 interfaces in perthites (Riedesel et al., 2021a). However, it is unknown whether lifetimes of the blue
84 emission are also affected by changes to the crystal structure. Previous research investigating lifetimes
85 of the blue emission indicated very fast decaying signals with lifetimes on the sub- μ s to few μ s-scale
86 (e.g. Clark et al., 1997; Clark and Bailiff, 1998). Besides those very fast lifetimes, Ankjærgaard and Jain
87 (2010) observed very long lifetimes for the blue emission on the ms- to s-scale. These authors suggest
88 band-tail state transport as the source of these long lifetimes.

89 For the yellow-green emission two likely defect sites have been proposed: (i) The emission at ~ 560 nm
90 has been assigned to Mn^{2+} substituting for Ca^{2+} in plagioclases resulting in a spin-forbidden transition
91 with long lifetimes on the ms-scale (e.g. Geake et al., 1971, 1973, 1977; Telfer and Walker, 1978); (ii)
92 Alternatively, the emission was suggested to result from Mn^{2+} substituting for Al^{3+} on tetrahedral sites
93 (T sites) in alkali feldspars, creating a lattice stabilising hole centre on $Si^{4+}-O-Mn^{2+}$ (Telfer and Walker,
94 1978; Kirsh et al., 1987). This second possibility would result in shorter lifetimes, due to the defect
95 being located at a lattice site. Clark and Bailiff (1998) have indeed observed very fast lifetimes (on the
96 ns-scale) for the emission at ~ 560 nm, supporting a lattice site defect for the yellow-green emission.
97 From phosphorescence data Prasad et al. (2016) observed dominant lifetimes of the yellow-green
98 emission of the order of hundreds of microseconds to less than a fraction of a millisecond – also an
99 observation against a spin forbidden transition of a defect located on cation sites (M sites). Riedesel et
100 al. (2021a) observed a strong yellow-green emission centred around 560 nm in alkali feldspar end
101 members albite and microcline, with all three samples having zero to negligible concentrations of MnO
102 as determined by x-ray fluorescence analysis. Thus, the source of the yellow-green emission in
103 chemically different alkali feldspars needs further investigation.

104 Besides using TR-luminescence to link certain defect types to luminescence emissions, feldspar TR-
105 luminescence has been used to improve the understanding of electron-hole recombination processes
106 and to infer possibilities to extract a more stable luminescence signal for dating. As part of this work,
107 it has been debated whether the TR-luminescence signal of feldspars represents the excited state
108 lifetime of the luminescence centre (the time needed for the electron to transition from the excited
109 state to the ground state of the luminescence centre, cf. e.g. Clark et al., 1997) or the recombination
110 lifetime (the time needed for the excited electron to move from the electron trapping centre to a
111 recombination centre) (e.g. Ankjærgaard et al., 2009; Tsukamoto et al., 2010), and which role band-
112 tail states play in this process (e.g. Jain and Ankjærgaard, 2011; Pagonis et al., 2012).

This is a **preprint**

The article has been submitted for peer-review to the *Journal of Luminescence* as:

Riedesel, S., Duller, G.A.T., Ankjærgaard, C., submitted. Time-resolved infrared stimulated luminescence of the blue and yellow-green emissions – insights into charge recombination in chemically and structurally different alkali feldspars. *Journal of Luminescence*.

113 The current understanding of feldspar luminescence is primarily based on a proximity model, where
114 the electron-hole pairs are separated by a distribution of distances and where it is understood that
115 recombination will occur at the nearest recombination centre (e.g. Huntley, 2006; Jain et al., 2012).
116 Feldspars containing a higher density of recombination centres will thus have less stable luminescence
117 signals, compared to feldspars with a lower density, because it will be more likely for electrons to
118 recombine at a proximal luminescence centre, even more likely through tunnelling processes (e.g.
119 Huntley, 2006; Jain et al., 2012). Subsequently, one would expect faster recombination lifetimes in a
120 system with a higher density of recombination centres, compared to systems with a lower
121 recombination centre density. Ankjærgaard et al. (2009) explored whether the TR-luminescence signal
122 of feldspars (green (532 nm) laser or blue (470 nm) LED stimulation and UV detection) reflected the
123 excited state or the recombination lifetime. They found arguments for either of the two processes
124 controlling the lifetimes measured. One argument supporting the recombination lifetime hypothesis
125 was shown by TR-OSL measured at different stimulation temperatures resulting in the same decay
126 shape, i.e. not giving rise to thermal quenching. However, Ankjærgaard et al. (2009) also found counter
127 arguments, thus supporting the excited state lifetime hypothesis: A systematic decrease in lifetime
128 with increasing preheat temperature was observed for feldspar TR-OSL. The authors argued that
129 longer lifetimes were expected for higher preheat temperatures, as a high preheat would result in a
130 depletion of recombination centres, making recombination more difficult and thus increasing the
131 recombination lifetime. Ankjærgaard et al. (2009) further explored whether different stimulation times
132 could affect the lifetimes and decay shape of the signals, expecting an increase in lifetimes with
133 increasing stimulation time. If the lifetimes measured would correspond to recombination lifetimes,
134 then one would expect longer lifetimes with decreasing hole concentrations due to longer stimulation
135 lifetimes. However, no clear trend was observed. Tsukamoto et al. (2010) compared TR-OSL and TR-
136 OSE (optically stimulated exo-electron) measurements of quartz, feldspar and NaCl and found that the
137 decay of TR-OSE signals are faster than TR-OSL in the case of NaCl and quartz, with TR-OSE signals
138 decaying on timescales $<1 \mu\text{s}$, while NaCl and quartz TR-OSL signals decay with a lifetime of $\sim 40 \mu\text{s}$. TR-
139 OSE and TR-OSL of feldspars decay on similar timescales. The very fast decaying TR-OSE signals are
140 understood as rapid emptying of the electron population in the conduction band immediately after
141 turning off the stimulation light source. In contrast, the slower decay of the TR-OSL signals is
142 interpreted as arising from relaxation processes within the recombination centre, thus being governed
143 by the excited state lifetime of these defects and the internal transitions.

144 Since the physical source of various TR-luminescence signals is still under debate, and it is still unclear
145 whether the off-time of TR-signals represents the excited or the recombination lifetime, different

This is a **preprint**

The article has been submitted for peer-review to the *Journal of Luminescence* as:

Riedesel, S., Duller, G.A.T., Ankjærgaard, C., submitted. Time-resolved infrared stimulated luminescence of the blue and yellow-green emissions – insights into charge recombination in chemically and structurally different alkali feldspars. *Journal of Luminescence*.

146 approaches have been used to describe TR-luminescence signals, particularly focussed on the off-time
147 signal. Most commonly a sum of multiple first order exponential functions have been used to describe
148 the TR off-time signal (e.g. Clark et al., 1997; Clark and Bailiff, 1998; Tsukamoto et al., 2006;
149 Ankjærgaard et al., 2009). However, feldspar luminescence is not a first order process (e.g. Huntley,
150 2006) and thus it has been proposed that fitting a sum of multiple first order exponential functions
151 might be inappropriate (e.g. Ankjærgaard, 2009; Pagonis et al., 2012, 2016). Jain and Ankjærgaard
152 (2011) thus visually separated the off-time signal into a “fast” and a “slow” TR-signal, with the “fast”
153 signal describing the initial decay, and the “slow” signal governing the TR-signal after 70 μ s in the off-
154 time. Pagonis et al. (2012) applied a linear combination of exponential and stretched exponential
155 functions. These authors interpreted the part of the TR-signal fitted by a stretched exponential as being
156 caused by transport via the band-tail states. Later Pagonis et al. (2016) developed analytical equations
157 describing feldspar TR-luminescence, which are based on the nearest-neighbour recombination model
158 by Jain et al. (2012). However, there are still many unknowns in the physical processes involved in
159 luminescence production in feldspars, so no definite answer can yet be given regarding the optimal
160 signal analysis procedure.

161 The research presented in this paper is focussed on creating a better understanding of defects and
162 processes involved in blue and yellow-green luminescence production. Therefore, we measure TR-
163 luminescence resulting from pulsed IR stimulation with emissions in the blue and yellow-green
164 wavelength region of a suite of representative single crystal alkali feldspars including single-phase
165 feldspars, perthites and artificially disordered feldspars. These are explored to investigate whether the
166 measured TR luminescence signal and its lifetimes and decay shape are governed by the recombination
167 or excited state lifetime and which role band-tail states might potentially play. We compare TR
168 luminescence resulting from different IRSL signals, different irradiation doses and of chemically and
169 structurally different feldspars.

170 **2 Materials and methods**

171 **2.1 Samples**

172 Samples investigated here are single crystal alkali feldspar specimens. Their chemical composition,
173 structural state and mineral phases present have been characterised previously and details can be
174 found in Riedesel et al. (2021a). The sample suite represents the chemical and structural range of the
175 alkali feldspar solid solution series and its end members. The chemical composition, mineral phases
176 present and the structural state of the samples was determined using x-ray fluorescence and x-ray
177 diffraction. FSM-13 is a single-phase microcline (98.5 % K-feldspar) and CLBR a single-phase albite (0.5

This is a **preprint**

The article has been submitted for peer-review to the *Journal of Luminescence* as:

Riedesel, S., Duller, G.A.T., Ankjærgaard, C., submitted. Time-resolved infrared stimulated luminescence of the blue and yellow-green emissions – insights into charge recombination in chemically and structurally different alkali feldspars. *Journal of Luminescence*.

178 % K-feldspar). FSM-3 (82.5 % K-FS), FSM-6 (74.4 % K-FS) and FSM-5 (74.8 % K-FS) are perthites. FSM-3
179 and FSM-6 are cryptoperthites consisting of albite and microcline (FSM-3) or orthoclase (FSM-6). FSM-
180 5 is a macropertthite consisting of albite and microcline. FSM-13LH and FSM-6LH are artificially
181 disordered samples. To obtain these samples, powdered sample material of FSM-13 and FSM-6 was
182 heated in Pt crucibles in a furnace to 1050 °C and then rapidly cooled to room temperature to retain
183 the disordered high-temperature structure, with Al³⁺ ions distributed randomly across tetrahedral sites
184 on the (Si,Al)-framework. Details of these experiments and a comparison of the x-ray diffraction
185 pattern of the ordered/disordered sample pairs can be found in Riedesel et al. (2021a). For each
186 sample three aliquots were measured.

187 **2.2 Instrumentation and measurement protocol**

188 Time-resolved luminescence measurements were made on a Risø TL/OSL DA20 reader equipped with
189 a ⁹⁰Sr/⁹⁰Y beta source delivering ~0.1 Gy s⁻¹ at the sample position and a Detection And Stimulation
190 Head (DASH) including an automated filter changer (Lapp et al. 2015). For the measurements
191 presented in this paper infrared stimulated luminescence (IRSL) was detected using a PDM 9107Q-AP-
192 TTL-03 (sensitive wavelength region: 160-630 nm) photomultiplier tube. For detection of the blue
193 emission (~410 nm) we used a combination of Schott BG39 (2 mm) and BG3 (3 mm) filters and for the
194 yellow-green emission (~550 nm) a combination of Schott BG39 (2 mm) and OG550 (2 mm) filters.
195 Dependent on the brightness of the sample ND 1.0 or ND 2.0 filters were added to the chosen filter
196 combination. The emission windows of the individual filters and the chosen filter combinations are
197 displayed in Figs. 1D and 1E. The stimulation was achieved using 850 nm (300 mW cm⁻²) IR LEDs,
198 operating at 90 % power.

199 Time-resolved luminescence measurements were possible through a photon timer attachment
200 (TimeHarp 260) in combination with the pulsed optically stimulated luminescence (OSL) unit (Lapp et
201 al., 2009). The TimeHarp 260 photon timer enables the detection of individual photons with a time
202 resolution of up to 1 ns. The pulsed IRSL plug-in board allows on- and off-times to be adjusted between
203 0.6 μs and 10 s. Additionally, different gating intervals can be selected. For time-resolved IRSL
204 measurements with emission detection in the blue wavelength region we used on-times of 50 μs,
205 followed by an off-time of 200 μs. Due to the much slower decay of the yellow-green time-resolved
206 IRSL signal, on-times were 5 ms, followed by an off-time of 45 ms. The time-resolved IRSL signals for
207 both emissions were recorded over a period of 200 s.

208 Time-resolved IRSL measurements were performed using a post-IR₅₀IRSL₂₂₅ protocol with a 60 s
209 preheat at 250 °C. The IR stimulation time was 200 s for the IRSL₅₀ and post-IR IRSL₂₂₅ signals. Prior to

This is a **preprint**

The article has been submitted for peer-review to the *Journal of Luminescence* as:

Riedesel, S., Duller, G.A.T., Ankjærgaard, C., submitted. Time-resolved infrared stimulated luminescence of the blue and yellow-green emissions – insights into charge recombination in chemically and structurally different alkali feldspars. *Journal of Luminescence*.

210 each measurement using the post-IR IRSL protocol the samples were annealed to 450 °C to ensure
211 complete signal resetting (Table 1). All samples were irradiated after the 450 °C clean-out. Blue time-
212 resolved IRSL measurements were performed after irradiation doses of 50, 200 and 800 Gy. Yellow-
213 green time-resolved IRSL measurements were conducted after doses of 200 or 800 Gy. In case of
214 samples FSM-5 and FSM-6 the yellow-green emission was not intense enough after a dose of 200 Gy,
215 thus these samples were irradiated with 400 Gy instead. Results of these dose-dependent
216 measurements are presented in section 3.1.3 for the blue emission. Results of these experiments for
217 the yellow-green emission are not shown, but results obtained from fitting are given in Tables S3a and
218 S3b in the supplementary material.

219

This is a **preprint**

The article has been submitted for peer-review to the *Journal of Luminescence* as:

Riedesel, S., Duller, G.A.T., Ankjærgaard, C., submitted. Time-resolved infrared stimulated luminescence of the blue and yellow-green emissions – insights into charge recombination in chemically and structurally different alkali feldspars. *Journal of Luminescence*.

220 *Table 1: Measurement protocol used.*

Step	Treatment	Purpose
1	TL to 450 °C, 1 °C s ⁻¹	Signal clean out
2	Beta dose 50, 200, 400 or 800 Gy	Irradiation, dose dependent on experiment
3	Preheat to 250 °C, 2 °C s ⁻¹ , 60 s	
4	IRSL ₅₀ , 2 °C s ⁻¹ , 200s Blue emission: 50 µs on-time, 200 µs off-time Yellow-green emission: 5 ms on-time, 45 ms off-time	Obtain time-resolved IRSL ₅₀ signal
5	post-IR IRSL ₂₂₅ , 2 °C s ⁻¹ , 200s Blue emission: 50 µs on-time, 200 µs off-time Yellow-green emission: 5 ms on-time, 45 ms off-time	Obtain time-resolved post-IR IRSL ₂₂₅ signal

221 Fitting of time-resolved luminescence signals was done in R using the nls() function (Bates and DeRoy,
222 2018) using equation 1 for the on-time signal and equation 2 for the off-time signal, where I is the
223 intensity at time t , A_i is the saturation intensity of the i 'th component and a_i the intensity at time t_1 ,
224 where t_1 is the on-time duration, and k is a constant, representing a stable linear background
225 (Chithambo, 2003; Tsukamoto et al., 2006). The data were normalised to the intensity of the last data
226 point of the on-time. The sole purpose of fitting the data was to enable a numerical comparison
227 between the samples used in this paper and to also be able to compare the data obtained here to
228 previously published time-resolved IRSL data (e.g. Clark and Bailiff, 1998; Tsukamoto et al., 2006,
229 2010). It is not our intention to make any suggestions regarding the physical processes by using the
230 numerical results obtained through fitting the data using a sum of multiple first order exponentials.
231 Later sections discussing potential physical properties of the samples and their influence on the TR-
232 luminescence signals are based on qualitative descriptions and sample-to-sample comparisons.

233
$$I(t) = \sum A_i \left[1 - \exp\left(\frac{-t}{\tau_i}\right) \right] \quad [1]$$

234
$$I(t) = \sum a_i \exp\left[-\left(\frac{t-t_1}{\tau_i}\right)\right] + k \quad [2]$$

This is a **preprint**

The article has been submitted for peer-review to the *Journal of Luminescence* as:

Riedesel, S., Duller, G.A.T., Ankjærgaard, C., submitted. Time-resolved infrared stimulated luminescence of the blue and yellow-green emissions – insights into charge recombination in chemically and structurally different alkali feldspars. *Journal of Luminescence*.

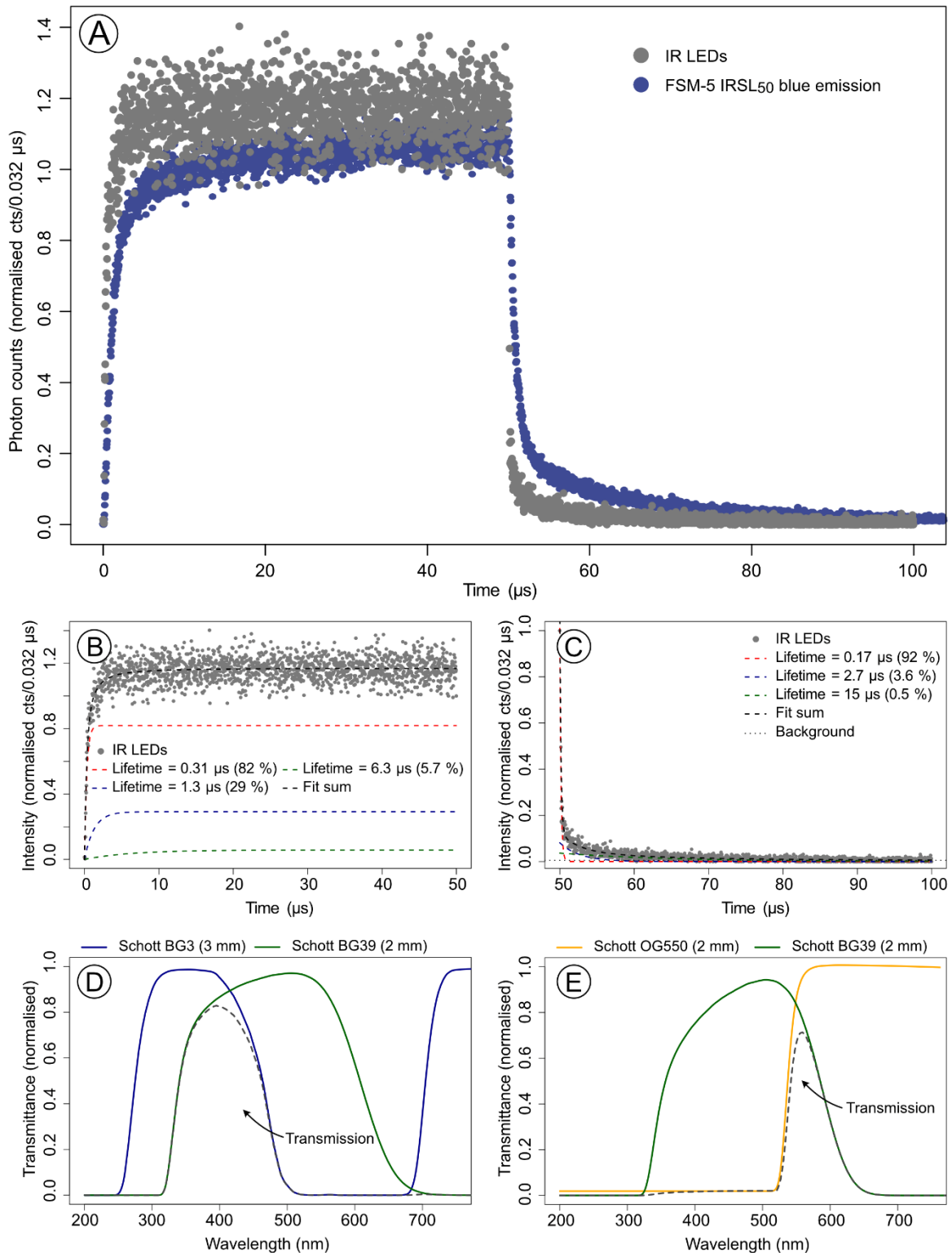


Fig. 1. A) The response of the IR LEDs measured through a ND filter for deadtime correction, and the signal was recorded using a red-sensitive photomultiplier tube (PMT). The signal of FSM-5, the fastest decaying signal from all samples measured, was recorded through the BG39 + BG3 combination visualised in D and was detected using a UV-sensitive PMT. This sample was chosen in comparison as it has the fastest decay in the off-time. B) Fitted LED on-time and C) off-time signal. The signal was normalised to the last point of the on-

This is a **preprint**

The article has been submitted for peer-review to the *Journal of Luminescence* as:

Riedesel, S., Duller, G.A.T., Ankjærgaard, C., submitted. Time-resolved infrared stimulated luminescence of the blue and yellow-green emissions – insights into charge recombination in chemically and structurally different alkali feldspars. *Journal of Luminescence*.

time, and the scatter of the data means that some measurement points lie above 1. D) Transmission of the BG3 and BG39 filter combination. E) Transmission of the OG550 and BG39 filter combination.

235

236 **3 Blue TR-IRSL emission – Results and Discussion**

237 The blue luminescence emission (~410 nm) is the emission commonly detected when using feldspars
238 for luminescence dating, thus this emission and potential variations of this emission between different
239 feldspars is of particular interest. In the following we investigate variations in the lifetimes of on- and
240 off-times of the blue TR-IRSL signals as a function of integration interval, irradiation dose, and IRSL
241 signal investigated. To enable a direct comparison all on- and off-time signals were fitted using a sum
242 of multiple first order exponential functions. We have also attempted to use a linear sum of single
243 exponential function and stretched exponential function (Pagonis et al., 2012) to describe our data.
244 However, fitting our data using the equation given by Pagonis et al. (2012) in R and SigmaPlot yielded
245 parameters values of infinity. The only samples we were able to fit using a linear sum of single
246 exponential function and stretched exponential function were the disordered samples FSM-13LH and
247 FSM-6LH. Thus, we only present lifetimes based on fitting with a linear sum of multiple first order
248 exponential functions.

249 **3.1 Lifetimes**

250 In the following we first investigate the effects of changing the integration interval, the IRSL signal
251 (IRSL₅₀ compared to post-IR IRSL₂₂₅) or the given dose on the on- and off-time lifetimes. To enable a
252 numerical comparison, we here use the results obtained from fitting using a sum of multiple
253 exponentials.

254 All results presented in the following sections are based on TR-luminescence signal fitting using
255 between one and four exponential functions (eq. 1 and 2). The number of components used for fitting
256 is based on the lowest residual signal obtained from fitting with different number of components,
257 thereby avoiding redundancy in the fitting. Using this approach, we obtained lifetimes ranging from
258 0.5 μ s to over 100 μ s. Faster lifetimes could not be detected due to the decay time of the IR LEDs (~0.3
259 μ s, cf. Fig. 1A, B, C). Generally, lifetimes could be arranged into three lifetime groups for the on-time
260 signal: <5 μ s, 8-20 μ s and > 20 μ s, and into four lifetime groups for the off-time: < 1 μ s, 3-9 μ s, 12-16
261 μ s and > 20 μ s. This grouping was done by identifying similar lifetimes between different samples and
262 the two signals investigated and are only used for visualisation purposes in figures and tables.
263 Differences in on- and off-time lifetimes might be related to the different time intervals used: 50 μ s
264 on-time compared to 200 μ s off-time, leading to an improved description of the longer off-time

This is a **preprint**

The article has been submitted for peer-review to the *Journal of Luminescence* as:

Riedesel, S., Duller, G.A.T., Ankjærgaard, C., submitted. Time-resolved infrared stimulated luminescence of the blue and yellow-green emissions – insights into charge recombination in chemically and structurally different alkali feldspars. *Journal of Luminescence*.

265 duration compared to the shorter on-time. All numerical fitting results can be obtained from the

266 supplementary material.

267

This is a **preprint**

The article has been submitted for peer-review to the *Journal of Luminescence* as:

Riedesel, S., Duller, G.A.T., Ankjærgaard, C., submitted. Time-resolved infrared stimulated luminescence of the blue and yellow-green emissions – insights into charge recombination in chemically and structurally different alkali feldspars. *Journal of Luminescence*.

268 ***Integration intervals***

269 The TR-IRSL signals were recorded over a stimulation period of 200 s, for the IRSL₅₀ and post-IR IRSL₂₂₅
270 signal, respectively. An example of IRSL decay curves measured during the on- and off-time is given for
271 sample FSM-13 in Fig. S1. Using the software PTanalyse, we extracted photon arrival time distributions
272 of the following time intervals for a comparison: 0-2 s, 0-5 s, 0-10 s, 0-50 s and 0-200 s, 10-50 s, 50-100
273 s and 100-200 s. To be able to make an absolute comparison, we selected two samples, FSM-3 and
274 CLBR, and fitted the extracted photon arrival time distributions of the on- and off-time of the IRSL₅₀
275 and post-IR IRSL₂₂₅ signals using equation 1 and 2. Figure S2 in the supplementary material shows the
276 results of FSM-3, results for CLBR are not shown, but are similar to those of FSM-3. We did not observe
277 any significant and consistent changes in lifetime with integration interval selected for either of the
278 IRSL signals or any samples. However, increasing the integrated time interval resulted in a better
279 goodness of fit, expressed as the square sum of residuals of the fit, with the best fit obtained when
280 integrating the photon arrival time distribution of the entire IRSL signal (total 200 s stimulation).
281 Subsequently, all data presented in this paper are based on whole IRSL signal integration.

282 ***Signals investigated – IRSL₅₀ compared to post-IR IRSL₂₂₅***

283 Post-IR IRSL signals are observed to be more stable compared to the IRSL₅₀ signal measured as part of
284 the post-IR IRSL protocol (e.g. Thomsen et al. 2008), likely due to the post-IR IRSL signal probing more
285 distant electron-hole-pairs (Jain and Ankjærgaard, 2011). TR-IRSL signal differences have also been
286 observed: Jain and Ankjærgaard (2011) defined a “fast” and a “slow” TR-signal and found different
287 behaviour of these two for the IRSL and post-IR IRSL signals measured in the UV at elevated
288 temperatures, and that the relative signal intensity between the fast and slow signal contribution
289 changes.

290 Here we compare lifetimes obtained for the two IRSL signals measured in the blue using a post-IR₅₀
291 IRSL₂₂₅ protocol. Figure 2 shows lifetimes of all samples obtained by fitting on- and off-time signals of
292 the IRSL₅₀ and post-IR IRSL₂₂₅. Figs. 2A and B show a direct comparison of all measured lifetimes and
293 their distribution around a 1:1 line, for the on- and off-times respectively. Especially at faster lifetimes
294 and in the off-time signal, IRSL₅₀ and post-IR IRSL₂₂₅ yield similar results and even the slower signals
295 show results scattered around the 1:1 line (Fig. 2 A, B). Sample-dependent lifetimes presented in Figs.
296 2C and D indicate variations in the presence of different lifetimes in the samples investigated. Further
297 details regarding sample-to-sample variations are discussed qualitatively in section 3.2. However, what
298 is also visible from Figs. 2C and D is that in some samples, some lifetimes only occur in either the IRSL₅₀

This is a **preprint**

The article has been submitted for peer-review to the *Journal of Luminescence* as:

Riedesel, S., Duller, G.A.T., Ankjærgaard, C., submitted. Time-resolved infrared stimulated luminescence of the blue and yellow-green emissions – insights into charge recombination in chemically and structurally different alkali feldspars. *Journal of Luminescence*.

299 or the post-IR IRSL₂₂₅ signal (e.g. Lifetime 1 in the on-time of sample FSM-6). Such points are not visible
300 from the diagrams in Figs. 2A and B. Despite these minor deviations and some observed variability, it
301 can be concluded that overall similar lifetimes can be obtained for all samples regardless of the IRSL
302 signal chosen.

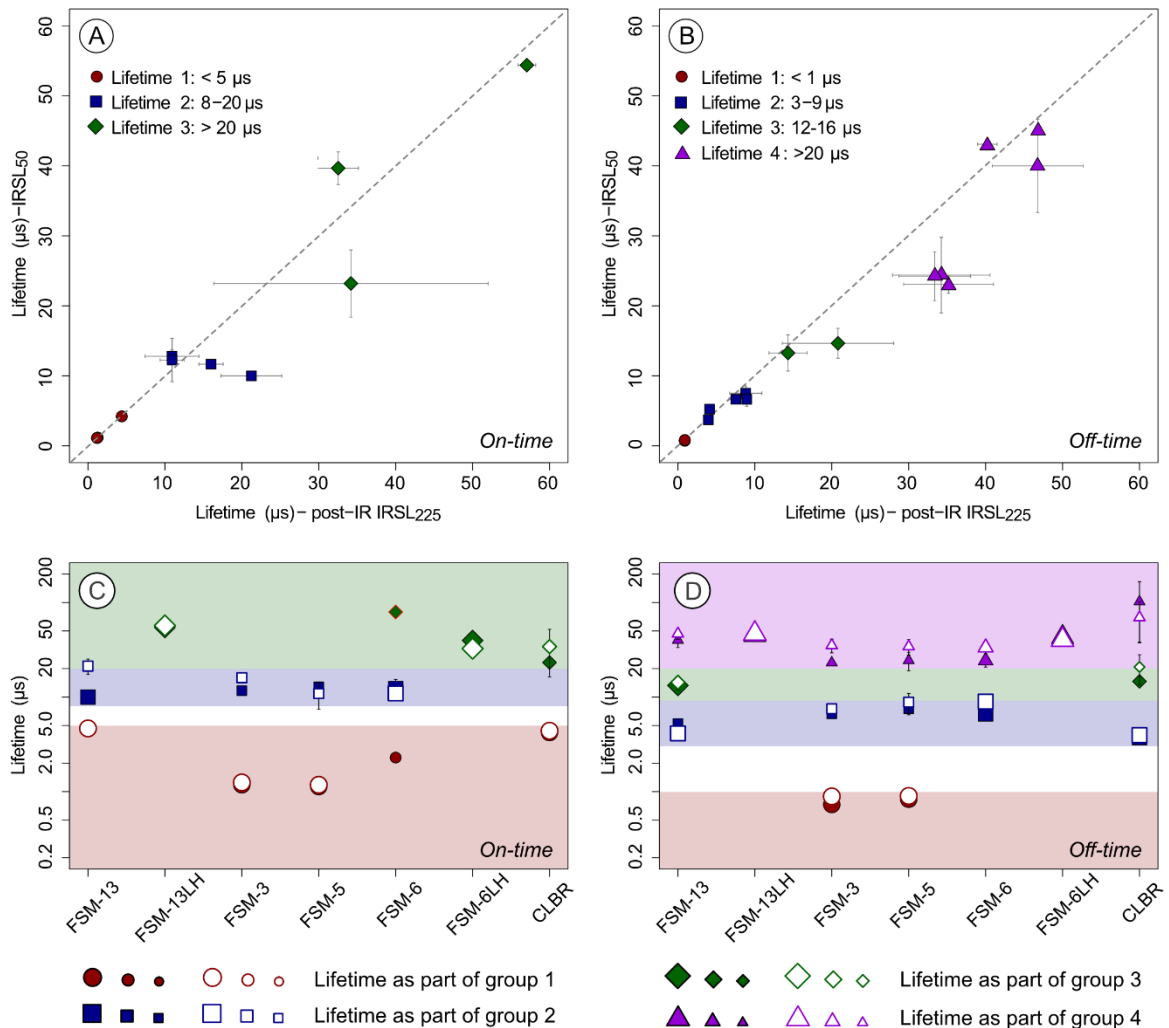


Fig. 2. Comparison of lifetimes obtained for the IRSL₅₀ and post-IR IRSL₂₂₅ signals for the on-time (A) and off-time (B) of the blue emission (50 Gy given dose). The dashed line in the graphs represent the one-to-one line. The data shown here is for all samples measured. The same data is shown in (C) and (D) where the fitted lifetime components are resolved for the individual samples. The data points in all figures represent the mean of three aliquots and their standard deviation. The diamond with red border (C) shows a lifetime, which only observed in one aliquot.

303

304 **Dose dependency**

305 Ankjærgaard et al. (2009) compared TR-OSL (470 nm LED and 532 nm laser stimulated) lifetimes
306 measured in the UV for different feldspars following irradiation doses of 5 Gy and 1000 Gy, dependent

307 on sample brightness, and showed that lifetime determination is independent of the dose
 308 administered. However, Ankjærgaard et al. (2009) did not explore IRSL or post-IR IRSL signals. Here we
 309 show the results of a systematic investigation of potential lifetime-dependencies for the blue emission
 310 (IRSL₅₀ and post-IR IRSL₂₂₅) for irradiation doses of 50 Gy, 200 Gy and 800 Gy (Fig. 3). The fitting results
 311 presented in direct comparison for the different doses in Fig. 3 scatter around the one-to-one line,
 312 indicating independence of the lifetimes of the doses given and thus supporting earlier work by
 313 Ankjærgaard et al. (2009) for OSL of feldspars.

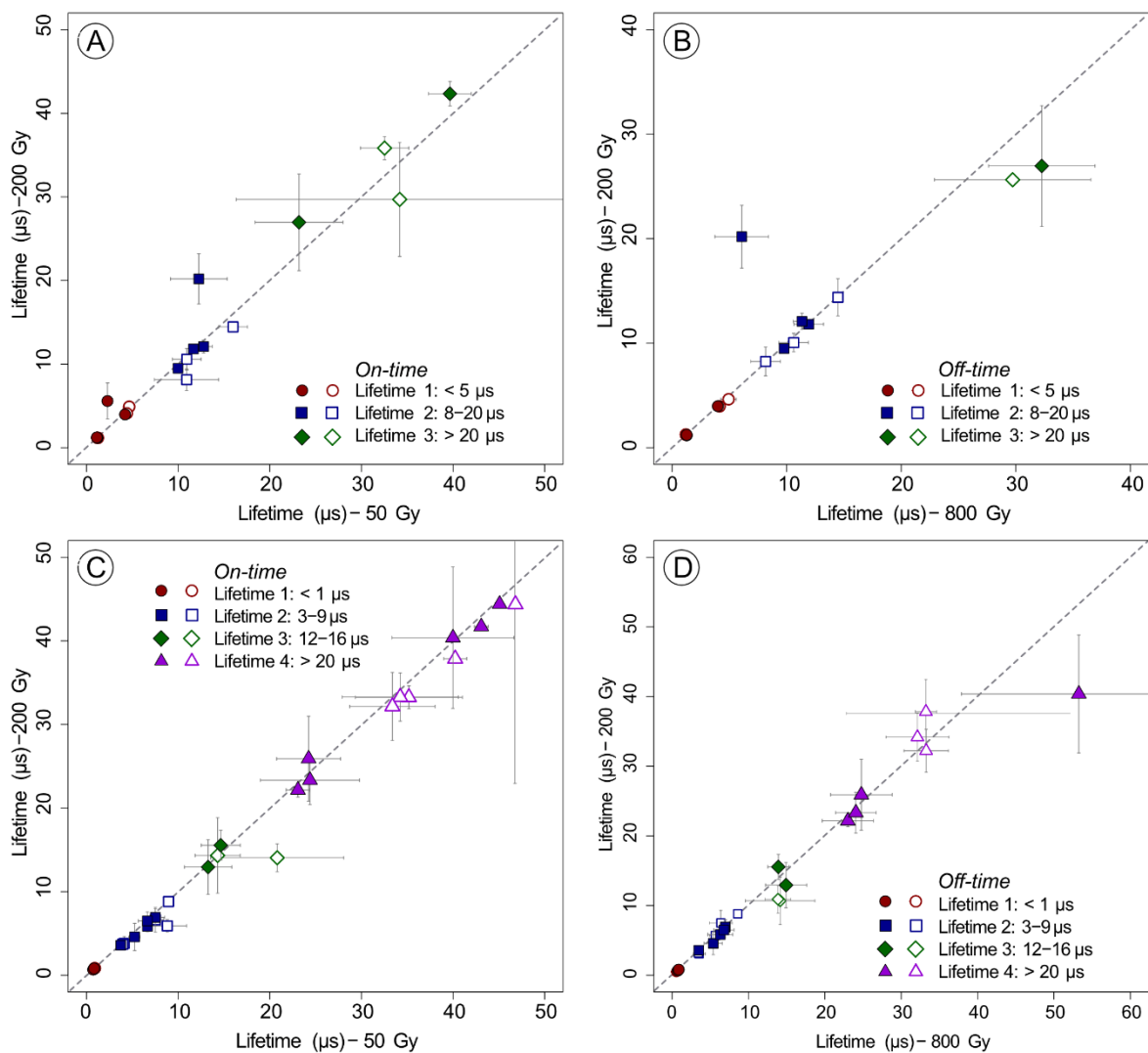


Fig. 3. Testing potential dose dependencies on the lifetimes of the IRSL₅₀ (filled symbols) and the post-IR IRSL₂₂₅ signal (open symbols) signal of the blue IRSL emission (on-time: A and B, off-time: C and D). Four doses were tested for this experiment, where the results of lifetimes obtained in response to 50 Gy are compared to 200 Gy (A and C) and 200 Gy are compared to 800 Gy (B and D).

314

315 **Lifetimes compared to literature values**

This is a **preprint**

The article has been submitted for peer-review to the *Journal of Luminescence* as:

Riedesel, S., Duller, G.A.T., Ankjærgaard, C., submitted. Time-resolved infrared stimulated luminescence of the blue and yellow-green emissions – insights into charge recombination in chemically and structurally different alkali feldspars. *Journal of Luminescence*.

316 Measurements performed in this paper resulted in lifetimes spanning the following time scales: On-
317 time: (1) $< 5 \mu\text{s}$, (2) $8\text{-}20 \mu\text{s}$, (3) $> 20 \mu\text{s}$. Off-time: (1) $< 1 \mu\text{s}$, (2) $3\text{-}9 \mu\text{s}$, (3) $12\text{-}16 \mu\text{s}$, (4) $> 20 \mu\text{s}$. These
318 lifetimes, obtained for the IRSL_{50} and post-IR IRSL_{225} signal, are in good agreement with previous work:
319 Clark and Bailiff (1998) presented very fast lifetimes of different emissions measured for various
320 chemically different feldspar samples using pulsed 850 nm laser stimulation. Their lifetimes range from
321 a few ns to the μs -scale. Due to instrumental limitations, we are unable to detect lifetimes faster than
322 $0.3 \mu\text{s}$, but lifetimes measured on the μs -scale in this paper are similar to those obtained by Clark and
323 Bailiff (1998). Using the sum of three exponential functions to describe the off-time decay, Tsukamoto
324 et al. (2006) measured blue IRSL lifetimes of 0.61, 2.4 and $19 \mu\text{s}$ for a Na-feldspar sample (grain
325 mixture) and 1.1, 4.3 and $19 \mu\text{s}$ for a K-feldspar sample (grain mixture). These values and the number
326 of exponentials used to describe the decay are similar to the results obtained in the present study (cf.
327 Fig. 2). Ankjærgaard et al. (2009) compared lifetimes of chemically different single crystal feldspars and
328 feldspar grain mixtures. These authors observed the UV emission of 532 nm laser and 470 nm diode
329 stimulated feldspars and enabled a comparison by using the sum of multiple first order exponentials
330 for fitting their off-time signals. The feldspars investigated showed lifetimes for the UV emission on
331 the μs -scale, with the fastest lifetimes ($<0.1 \mu\text{s}$) obtained through pulsed 532 nm laser stimulation.
332 Longest lifetimes measured ranged from $\sim 10 \mu\text{s}$ to $<100 \mu\text{s}$, and are thus within the range of lifetimes
333 obtained in the present study, but it should be noted that stimulation and emission wavelengths differ
334 from our study.

335 ***Excited state vs. recombination lifetime?***

336 Here we compared lifetimes of different feldspars, measured using two different IRSL signals, obtained
337 from different IRSL integration intervals, and after different irradiation doses. Figs. 2 and 3, and Fig. S1
338 showed that the lifetimes seem to be largely independent of the given dose, the signal integration
339 interval and IRSL signal measured. This observation is in support of the excited state lifetime hypothesis
340 if one assumes a random distribution of donor and acceptor pairs in a proximity model. However, the
341 recombination lifetime might still be considered as a valid explanation, if the defect density is so high
342 that changes to e.g. the number of populated defects through different doses might be so small that
343 changes to the lifetime cannot be observed.

344 **3.2 Sample-to-samples variations in the blue time-resolved IRSL_{50} signal**

345 We showed in section 3.1 that neither the on- nor the off-time of the blue IRSL signal depends on the
346 IRSL signal integration interval, or the dose given. We also showed that the IRSL_{50} signal and the post-

347 IR IRSL₂₂₅ signal result in similar lifetimes. Thus, these findings support the excited state lifetime
 348 hypothesis, unless the defect density is too high to observe any potential changes of the populated
 349 defects and their effect on the lifetimes. In the following we investigate TR-IRSL (blue emission) of a
 350 suite of chemically and structurally well-constrained alkali feldspars for which previous studies
 351 (Riedesel et al., 2021a) have demonstrated how their different compositions and structure impact the
 352 blue and infrared luminescence emissions and fading rates. This will enable us to study variations in
 353 TR-luminescence signals and their potential physical causes. Since no dependence on dose and IRSL
 354 signal investigated were found in the previous experiments all results shown in the following are based
 355 on the IRSL₅₀ signal which was recorded after a dose of 200 Gy. The discussion is based on qualitative
 356 comparisons between samples, as we will make some statements regarding potential physical
 357 processes in feldspars. Except in cases where time-resolved signals can be fitted using a single
 358 exponential function, no quantitative assessments are made, to avoid confusion about the kinetic
 359 order of feldspar luminescence.

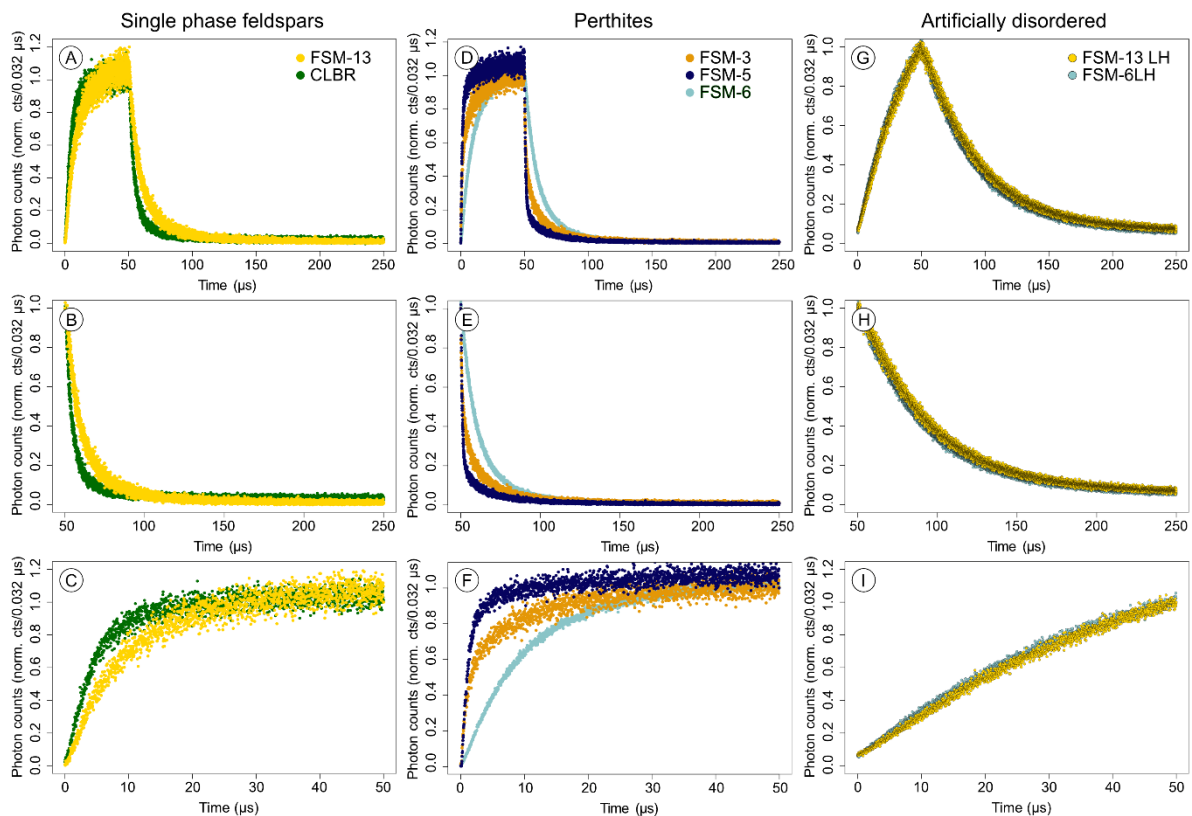


Fig. 4. Time-resolved IRSL₅₀ of the blue emission (200 Gy) for single phase feldspars, perthites and artificially disordered samples. A, D and G show the whole signals, B, E and H the off-time signal and C, F and I the on-time.

360

This is a **preprint**

The article has been submitted for peer-review to the *Journal of Luminescence* as:

Riedesel, S., Duller, G.A.T., Ankjærgaard, C., submitted. Time-resolved infrared stimulated luminescence of the blue and yellow-green emissions – insights into charge recombination in chemically and structurally different alkali feldspars. *Journal of Luminescence*.

361 Figure 4 shows a comparison of blue time-resolved IRSL₅₀ signals obtained for the different samples.
362 For the seven feldspars investigated we observed a range of different TR-luminescence signals. Whilst
363 all samples show an on-time signal increase and an off-time decay on the μ s-scale, there are subtle
364 differences between samples. The fastest rise and decay can be found in macroperthite FSM-5 (Fig.
365 4D-F), followed by K-rich cryptoperthite FSM-3, where the short lifetime components appear to be
366 dominating the shape. Perthitic sample FSM-6 and the two single phase feldspars microcline FSM-13
367 and albite CLBR show similar TR-signals, although CLBR shows faster signal increase and decay
368 compared to FSM-13 (Fig. 4A-C). The slowest rise and decay of the TR-IRSL signal can be found in the
369 two artificially disordered feldspars FSM-13LH and FSM-6LH (Fig. 4G-I), where the longer lifetime
370 components appear to be dominating the shape. A direct comparison between the artificially
371 disordered samples FSM-13LH and FSM-6LH and their ordered counterparts is shown in Figure 5. When
372 comparing the artificially disordered samples FSM-13LH and FSM-6LH it is evident that the two samples
373 show very similar on- and off-time signal behaviour, with samples FSM-6LH showing only slightly faster
374 signals. Fitting of the TR-luminescence signals of these two artificially disordered samples was possible
375 by using a single exponential function plus a constant background signal (i.e. k in eq. 2) and lifetimes
376 obtained are around $\sim 45 \mu$ s.

This is a **preprint**

The article has been submitted for peer-review to the *Journal of Luminescence* as:

Riedesel, S., Duller, G.A.T., Ankjær, C., submitted. Time-resolved infrared stimulated luminescence of the blue and yellow-green emissions – insights into charge recombination in chemically and structurally different alkali feldspars. *Journal of Luminescence*.

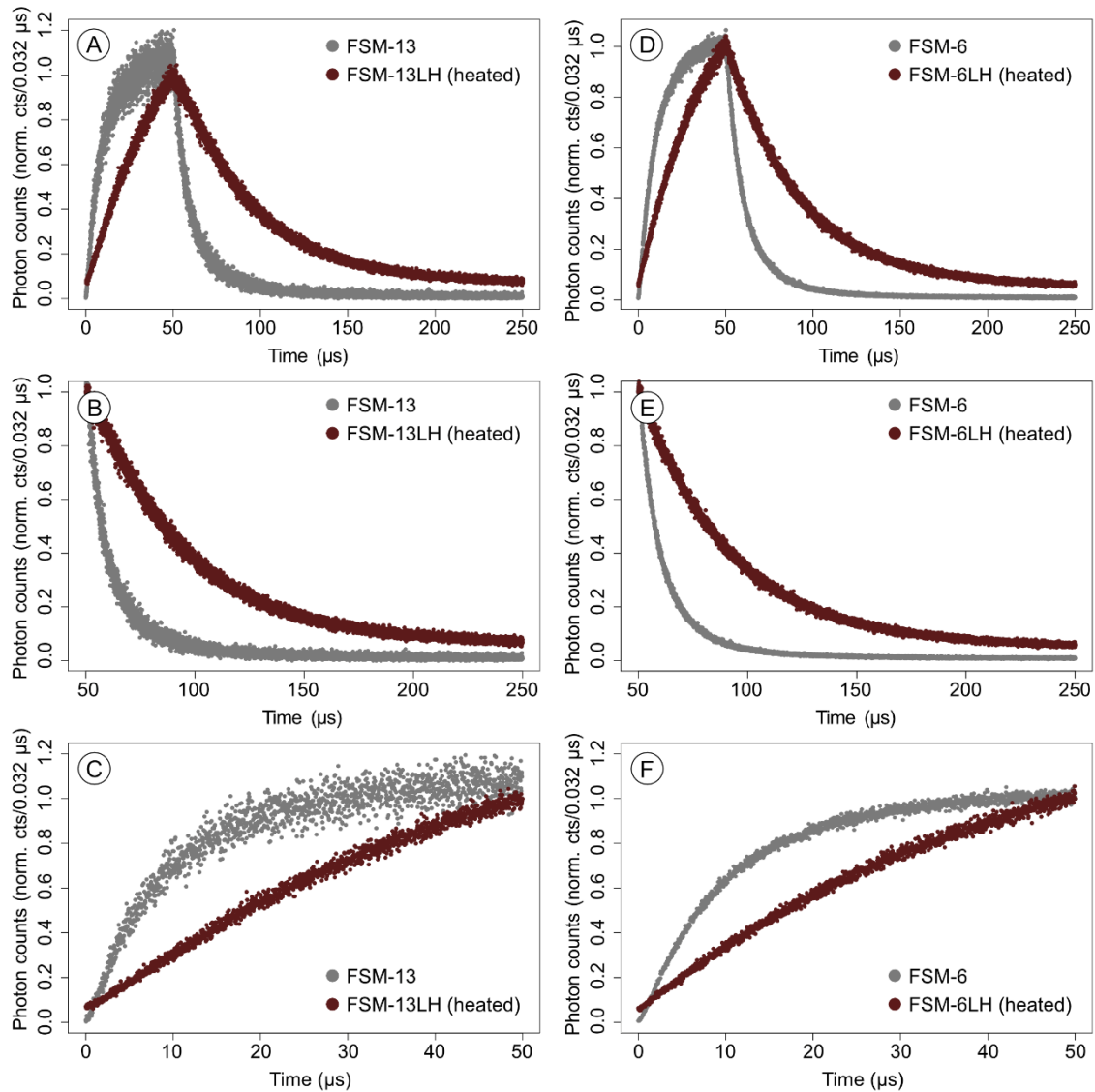


Fig. 5. Time resolved signals of the blue IRSL₅₀ emissions (200 Gy) of unheated and heated sample pairs FSM-13 and FSM-13LH (A, B, C) and FSM-6 and FSM-6LH (D, E, F).

377

378 This slow rise and decay and the lifetimes obtained from fitting using a single exponential function are
379 similar to results obtained for quartz elsewhere (e.g. Bailiff, 2000; Chithambo 2003; 2007). One other
380 feature of quartz TR-luminescence signals is a significant decrease in lifetime with increasing
381 stimulation temperature, which has been associated with thermal quenching (Bailiff, 2000; Chithambo,
382 2003). Bailiff (2000) observed a decrease in the decay lifetime of synthetic quartz from ~40 μs to 8 μs,
383 when increasing the stimulation temperature from room temperature to 210 °C. These observations
384 are supported by similar experiments made by Chithambo (2003) on natural sand-sized quartz. To test
385 potential influence from thermal quenching on lifetimes and TR-luminescence signals of artificially
386 disordered feldspars, we measured TR-IRSL signals at different stimulation temperatures. The signals

387 were recorded using the protocol described in Table 1. We varied the stimulation temperature of the
388 post-IR IRSL signal (step 5 in Table 1) from 50 °C to 225 °C in 25 °C steps. In contrast to observations
389 made on quartz, our artificially disordered feldspars do not show thermal quenching (cf. Fig. 6) and
390 lifetimes measured remain at a constant level around ~45 μ s. Thus, we conclude that artificially
391 disordering influences the lifetime of the blue emission, however, the resulting emission and related
392 processes seem to differ from what has been observed for quartz, and thus do not show any thermal
393 quenching effects.

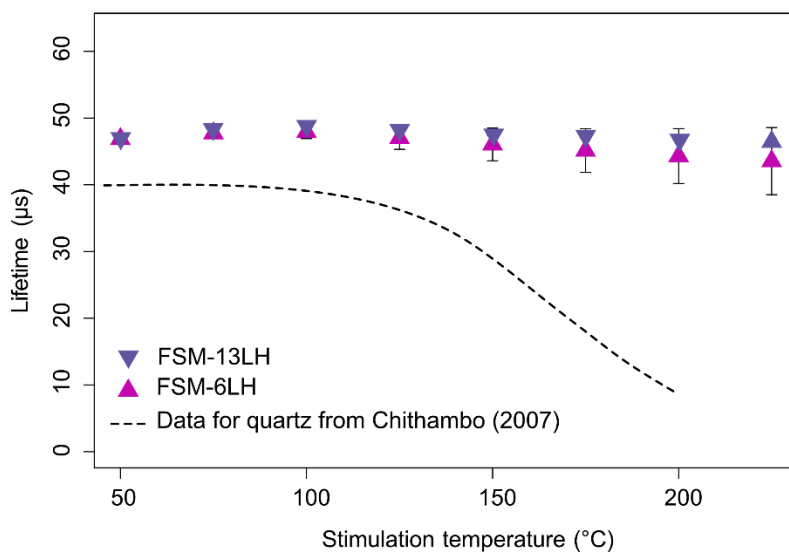


Fig. 6. Effect of varying the stimulation temperature of the post-IR IRSL signal on the lifetimes of the second IRSL signal in the post-IR₅₀ IRSL₅₀₋₂₂₅ °C protocol on disordered (heated) samples FSM-13LH and FSM-6LH. The lifetimes are compared to data obtained from quartz (Chithambo, 2007). Data points from this study represent the average and standard deviation of measurements of three aliquots.

394

395 The sample-to-sample variations in rise and decay of the TR-IRSL signals are striking, particularly
396 showcasing the changes observed for the ordered and disordered samples pairs. Whilst we observe
397 these variations in TR-signals, we so far cannot explain what causes these. However, these samples
398 have been investigated previously and thus some information regarding their luminescence
399 characteristics are known, enabling potential links between existing information and the newly
400 gathered time-resolved results.

401 When comparing TL emission spectra and fading rates of the same single-phase feldspars and perthites
402 as explored in the present study, Riedesel et al. (2021a) observed differences in emission intensities
403 and fading rates of the samples investigated. Whilst single-phase feldspars (microcline and albite) only
404 showed weak blue luminescence and no fading, cryptoperthites were characterised to have intense
405 and broad blue emissions and fading rates ranging from ~2 to ~7 %/decade. Macroperthites exhibited

This is a **preprint**

The article has been submitted for peer-review to the *Journal of Luminescence* as:

Riedesel, S., Duller, G.A.T., Ankjærgaard, C., submitted. Time-resolved infrared stimulated luminescence of the blue and yellow-green emissions – insights into charge recombination in chemically and structurally different alkali feldspars. *Journal of Luminescence*.

406 the highest fading rates with up to 12 %/decade. Riedesel et al. (2021a) found that these observations
407 support a location for the defect responsible for the blue emission on Al-O-Al bridges (cf. Finch and
408 Klein, 1999). The data presented by Riedesel et al. (2021a) suggests that potentially higher densities of
409 these defects can be found along the interfaces in perthites. TR-IRSL measurements of single-phase
410 feldspars, albite (CLBR) and microcline (FSM-13), and perthites (FSM-3, FSM-5 and FSM-6), revealed
411 slightly slower TR-IRSL on-time rise and off-time signal decay for single-phase feldspars compared to
412 perthites (Fig. 4A-C compared with Fig. 4D-F). Macroperthite FSM-5 shows the fastest signals.
413 However, perthite FSM-3 shows very similar TR-IRSL signals when comparing it to the two single-phase
414 feldspars investigated. This suggests that either the excited state lifetime of the recombination centre
415 is similar in perthites and single-phase albite and microcline or that the recombination lifetimes are on
416 similar time scales. The latter would then suggest similar recombination routes and likely similar defect
417 concentrations in these different feldspars. However, this is not reflected by the blue TL emission
418 intensities and fading rates observed by Riedesel et al. (2021a).

419 Riedesel et al. (2021a) compared TL emission spectra and fading rates of the same ordered and
420 disordered sample pairs as investigated here. They found that the blue luminescence emission
421 intensity and the IRSL fading rate increased with framework disorder. This was interpreted as the result
422 of an increase in recombination centre density due to framework disorder. A denser defect population
423 would, if the recombination lifetime hypothesis holds true, result in a faster TR signal. However, the
424 contrary is observed here (cf. Fig. 5), potentially indicating a change in the blue luminescence centre
425 properties and thus a change to the excited state lifetime of this luminescence centre.

426 Whilst large differences in fading rate and blue luminescence emission intensity were found across
427 different feldspars, electron trapping centres, understood to be involved in feldspar IRSL (e.g. Prasad
428 et al., 2017; Kumar et al. 2018), seem to be largely independent of changes to the sample chemistry or
429 structure (Riedesel et al., 2019, 2021b). Riedesel et al. (2019, 2021b) showed that the electron trapping
430 centre depth as well as emissions related to trapping and retrapping at electron trapping centres are
431 similar across the alkali feldspar group.

432 If the electron trapping centres are independent of the sample's chemistry or structural state, then
433 changes in lifetime of the blue luminescence emission in ordered and disordered sample pairs and
434 across the chemical range of alkali feldspars, are either related to changes in the blue luminescence
435 centre itself or to parts of the crystal unrelated to electron trapping centres. Ankjærgaard and Jain
436 (2010) and Jain and Ankjærgaard (2011) suggested that the slower part of the TR decay could result
437 from recombination via the band-tail states. Pagonis et al. (2012) further investigated this hypothesis

This is a **preprint**

The article has been submitted for peer-review to the *Journal of Luminescence* as:

Riedesel, S., Duller, G.A.T., Ankjærgaard, C., submitted. Time-resolved infrared stimulated luminescence of the blue and yellow-green emissions – insights into charge recombination in chemically and structurally different alkali feldspars. *Journal of Luminescence*.

438 by exploring TR-IRSL of four feldspar museum specimens. Pagonis et al. (2012) applied a fitting
439 approach which combined a single exponential and a stretched exponential function, where the
440 authors related the results of the stretched exponential to the band-tail states. The observed increase
441 in TR-IRSL lifetime with increasing disorder of the framework in this paper could be related to a higher
442 density of band-tail states or a wider band-tail due to disorder of the crystal. A wider or denser sub-
443 conduction band tail could potentially result in an increased transport of charge via these states –
444 resulting in slower recombination processes than would be expected for excited state tunnelling (cf.
445 Jain and Ankjærgaard, 2011).

446 **4 Yellow-green TR-IRSL emission – Results and Discussion**

447 The yellow-green emission is rarely used in luminescence dating applications, however, it has been
448 identified as a common emission in many plagioclase feldspars (e.g. Geake et al., 1971, 1973, 1977;
449 Telfer and Walker, 1978), and was also recorded in microcline samples (c.f. Rendell and Clarke, 1997;
450 Riedesel et al., 2021a). Whilst being present as a distinct emission in some samples, the broad emission
451 recorded for perthites often spans from the blue into the yellow wavelength region (cf. Riedesel et al.,
452 2021a) and might thus include this emission. Two potential defects have been proposed for causing
453 this emission: (i) Mn^{2+} substituting for Ca^{2+} on M sites (e.g. Geake et al., 1971, 1973, 1977; Telfer and
454 Walker, 1978) or (ii) Mn^{2+} substituting for Al^{3+} on T sites (Telfer and Walker, 1978; Kirsh et al., 1987;
455 Clark and Bailiff, 1998). In the following we show the recorded TR-IRSL signals for the yellow-green
456 emission and the sample-to-sample variations we observed for this emission. The results shown in this
457 section are based on TR measurements of the IRSL₅₀ signal, measured after an irradiation dose of 200
458 Gy (or 400 Gy, in case of FSM-5 and FSM-6).

This is a **preprint**

The article has been submitted for peer-review to the *Journal of Luminescence* as:

Riedesel, S., Duller, G.A.T., Ankjærgaard, C., submitted. Time-resolved infrared stimulated luminescence of the blue and yellow-green emissions – insights into charge recombination in chemically and structurally different alkali feldspars. *Journal of Luminescence*.

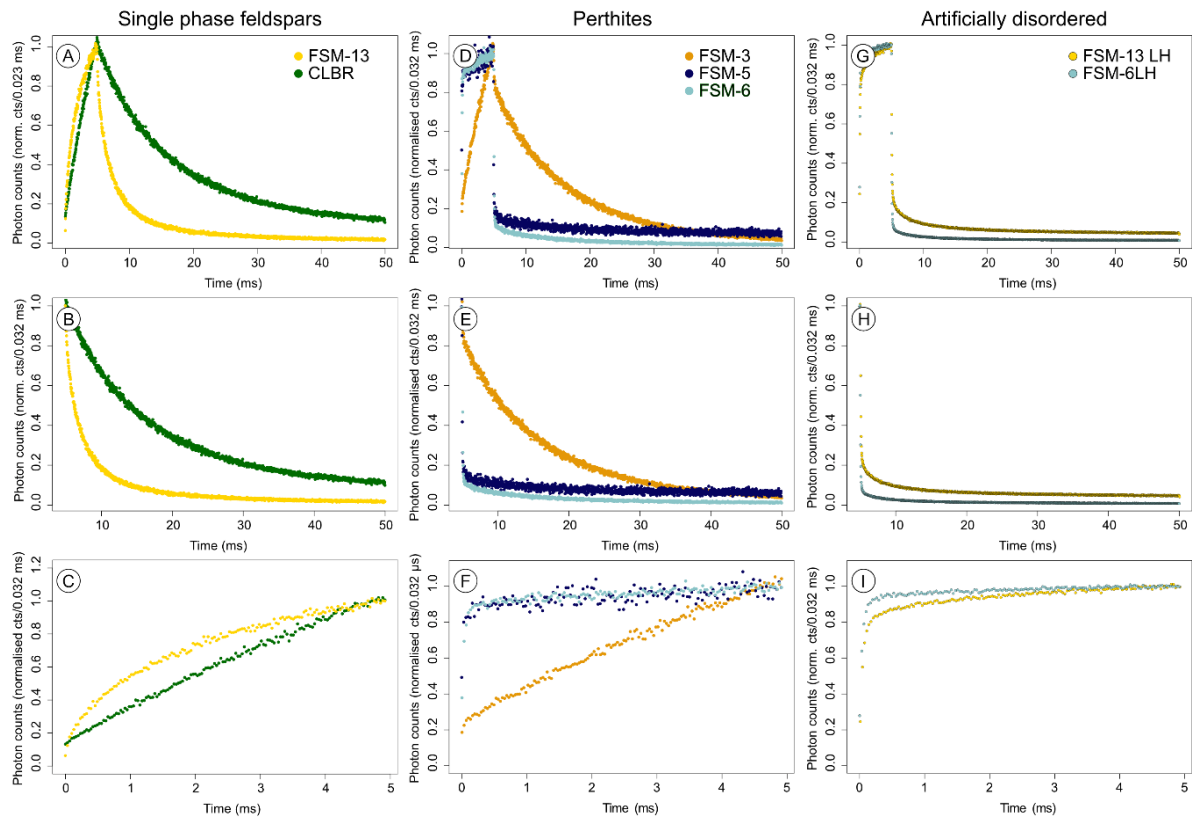


Fig. 7. Time-resolved IRSL₅₀ of the yellow-green emission for single phase feldspars, perthites and artificially disordered samples. The signals were recorded after an irradiation dose of 200 Gy (400 Gy in case of FSM-5 and FSM-6). A, D and G show the whole signals, B, E and H the off-time signal and C, F and I the on-time.

459

460 For all samples we observed TR-IRSL signals on the ms-scale (Fig. 7), which is much slower compared
461 to most of the observations made for the blue emission (Fig. 8). However, the different samples contain
462 varying proportions of the slower part of the TR signal. Especially in perthitic and disordered samples
463 the yellow-green emission is dominated by a very fast component, visible by the sharp increase at the
464 beginning of the on-time and the sharp decrease at the start of the off-time (cf. Figs. 7 D-I). TR on- and
465 off-time signals of single-phase feldspars FSM-13 and CLBR and perthite FSM-3 are significantly slower
466 compared to the other samples (cf. Fig. 7A-C, D-F).

This is a **preprint**

The article has been submitted for peer-review to the *Journal of Luminescence* as:

Riedesel, S., Duller, G.A.T., Ankjærgaard, C., submitted. Time-resolved infrared stimulated luminescence of the blue and yellow-green emissions – insights into charge recombination in chemically and structurally different alkali feldspars. *Journal of Luminescence*.

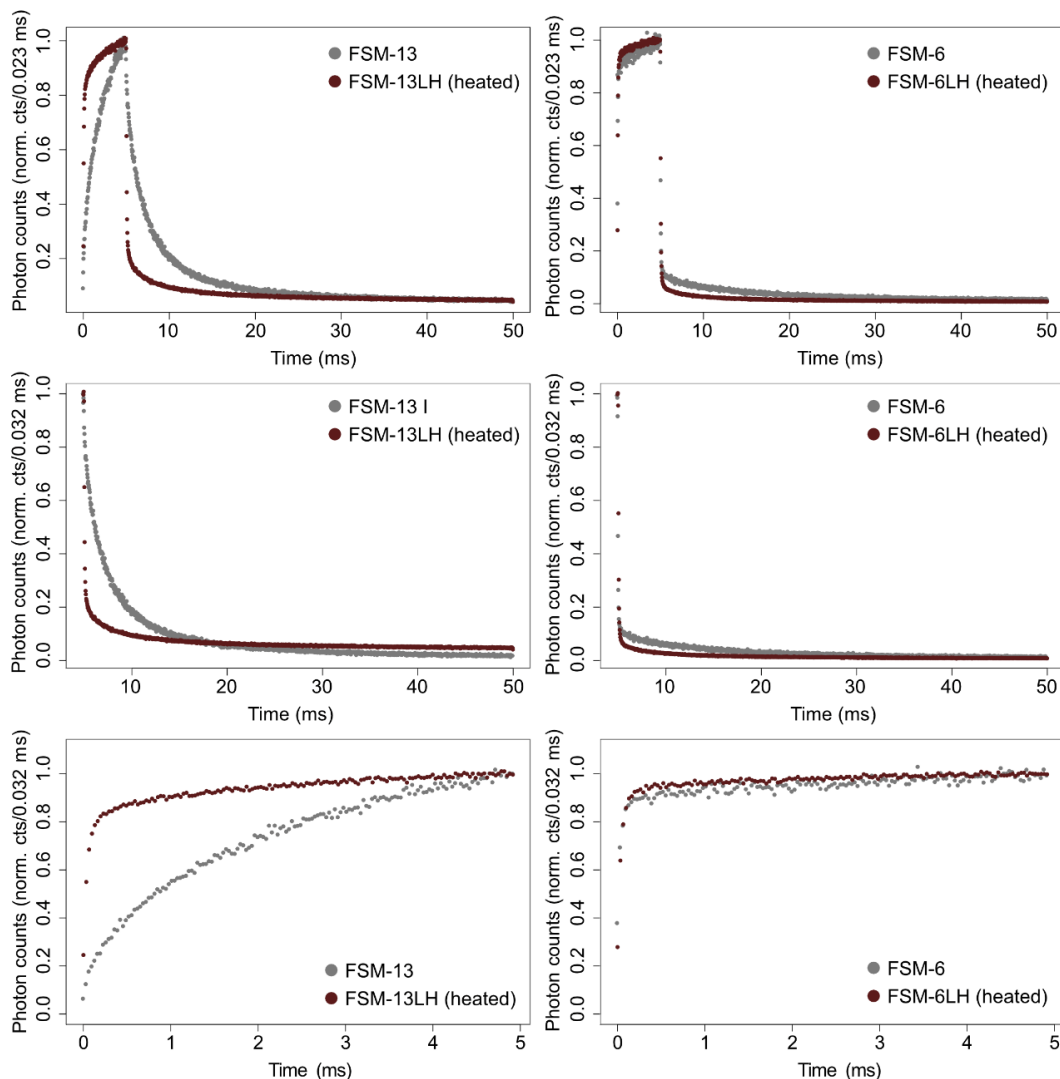


Fig. 8. Time resolved signals of the yellow-green $IRSL_{50}$ emissions of unheated and heated sample pairs FSM-13 and FSM-13LH (heated) (A, B, C) and FSM-6 and FSM-6LH (heated) (D, E, F).

467

468 A comparison of the ordered and disordered sample pairs reveals that the yellow-green emission
469 becomes faster during the on- and off-time when the sample is disordered (Fig. 8). The effect is more
470 visible in the case of FSM-13 and FSM-13LH, compared to FSM-6 and FSM-6LH. However, from TL
471 emission spectra it becomes apparent that disordering results in a significant increase in blue TL
472 emission intensity (Riedesel et al., 2021a). This could potentially result in breakthrough of this strong
473 blue emission into the emission window we used to record the yellow-green emission. This might also
474 explain the fast initial rise and decay in samples FSM-3 and FSM-5. Alternatively, the fast signals
475 recorded for the yellow-green emission could originate from the defect being located on a tetrahedral
476 site, as previously suggested by Clark and Bailiff (1998). These authors observed very fast lifetimes for
477 the yellow-green emission, even on the ns-scale, when fitting their TR-signals.

This is a **preprint**

The article has been submitted for peer-review to the *Journal of Luminescence* as:

Riedesel, S., Duller, G.A.T., Ankjærgaard, C., submitted. Time-resolved infrared stimulated luminescence of the blue and yellow-green emissions – insights into charge recombination in chemically and structurally different alkali feldspars. *Journal of Luminescence*.

478 Whilst we proposed a potential influence of band-tail states as the explanation for longer lifetimes of
479 the blue emission in disordered samples, this hypothesis would not hold in case of the yellow-green
480 emission, as the slowest signal rise and decay is found in ordered end member samples.

481 Observing significant differences in the time scale of signal rise and decay could indicate that the
482 emission indeed results from two different defect types. Long lifetimes obtained here for single-phase
483 microcline FSM-13 and albite CLBR suggest a metal ion site defect as source of the yellow-green
484 emission, even in alkali feldspars, supporting the Mn^{2+} substituting for Ca^{2+} on M site hypothesis by
485 e.g. Telfer and Walker (1978). In this case, a spin-forbidden transition would explain the lifetimes on
486 the ms-scale. However, short lifetimes (μs -scale) would be expected for a defect resulting from Mn^{2+}
487 substituting for Al^{3+} on T sites (cf. Clark and Bailiff, 1998). In this case the defect responsible for the
488 yellow-green emission would be a lattice stabilising hole centre on $Si^{4+}-O^- - Mn^{2+}$, as the hole centre on
489 the O ion would help in charge neutralisation, due to the introduced imbalance by Mn^{2+} substituting
490 for Al^{3+} (Telfer and Walker, 1978; Kirsh et al., 1987). If this type of defect is indeed present in our
491 samples, then one would expect that framework disorder influences the lifetime of this signal, as is
492 also shown in Fig. 8. Unfortunately, we cannot completely rule out any influence of breakthrough of
493 the blue emission, so no definite answer can be given here. However, it is striking that the strong
494 yellow-green emission can be found in the single-phase microcline, which also shows on-time increase
495 and off-time decrease in TR-IRSL measurements on similar time-scales as seen for the albite specimen.
496 This could indicate that whatever the type of defect, it is not restricted to plagioclase feldspars and
497 might thus not be Mn^{2+} substituting for Ca^{2+} on M sites.

498 **5 Conclusions**

499 In this paper we presented time-resolved infrared stimulated luminescence signals measured for a
500 range of single crystal alkali feldspars, including K- and Na-feldspar end members (microcline and
501 albite, both single phase), for the blue emission (~ 410 nm) and the yellow-green emission (~ 550 nm)
502 using a post- IR_{50} IRSL₂₂₅ protocol. The timescale on which the blue and the yellow-green emissions
503 occur differ significantly; the blue signal on the μs -scale, and the yellow-green emission on the ms-
504 scale. For each emission the lifetimes are independent of the signal integration interval, the IRSL signal
505 investigated, and the dose given.

506 For the blue emission there is a slight difference in decay time scale between single-phase feldspars
507 and perthites, however more significant differences are observed when the feldspars are artificially
508 disordered. Our new observations show that artificially disordering the framework significantly

This is a **preprint**

The article has been submitted for peer-review to the *Journal of Luminescence* as:

Riedesel, S., Duller, G.A.T., Ankjærgaard, C., submitted. Time-resolved infrared stimulated luminescence of the blue and yellow-green emissions – insights into charge recombination in chemically and structurally different alkali feldspars. *Journal of Luminescence*.

509 increases the rise and decay time of the on- and off-time, and that the signals can now be described
510 using a single exponential fit. The lifetimes obtained from the disordered feldspars are similar to those
511 measured for quartz elsewhere (c.f. Bailiff 2000, Chithambo 2003), but unlike the quartz signals the
512 TR-signals here do not show any thermal quenching. The longer lifetimes observed for disordered
513 feldspars could (i) either result from a change of the blue recombination centre, resulting in longer
514 excited state lifetimes of the defect itself, (ii) or increased disorder of the lattice could cause changes
515 to the band-tail state width or density, increasing the likelihood of recombination occurring via the
516 band-tail states, resulting in longer recombination lifetimes (c.f. Jain and Ankjærgaard, 2011; Pagonis
517 et al., 2012).

518 Time-resolved signals of the yellow-green emission vary between samples, with single-phase
519 microcline and albite specimens showing the slowest signals. These slow time scales could indicate a
520 spin-forbidden transition, as has been proposed for a defect resulting from Mn²⁺ substituting for Ca²⁺
521 on M sites. However, the Ca content of the microcline specimen is negligible and the Mn content so
522 low that it could not be detected.

523 In contrast to slow signals in the single-phase samples, perthitic and disordered samples show a large
524 proportion of a fast signal decay in the off-time, before a slow component describes the remaining
525 part of the TR-signal. The fast signal could either indicate a different type of defect for this emission
526 or, alternatively, it could be an artefact resulting from breakthrough of the blue emission. This needs
527 further investigation in future measurements.

528 The data in this paper shows the potential for using time-resolved IRSL to gain information on the
529 structural state of the feldspar investigated and thus helping in understanding variations in
530 luminescence properties across a range of chemically and structurally different feldspars.

531 **Acknowledgements**

532 Initial TR-luminescence measurements, which formed the basis for the research presented in this
533 paper, were performed during SR's PhD at Aberystwyth University. SR's PhD research was funded
534 through an AberDoc PhD scholarship by Aberystwyth University. We would like to thank Hollie Wynne
535 (Aberystwyth University) for preparing the aliquots for all measurements, so that SR could run the
536 experiments remotely during the Covid-19 pandemic. We would like to thank Anthony M.T. Bell
537 (Sheffield Hallam University) for performing XRF and XRD measurements, characterising the feldspar
538 samples used in this study.

This is a **preprint**

The article has been submitted for peer-review to the *Journal of Luminescence* as:

Riedesel, S., Duller, G.A.T., Ankjærgaard, C., submitted. Time-resolved infrared stimulated luminescence of the blue and yellow-green emissions – insights into charge recombination in chemically and structurally different alkali feldspars. *Journal of Luminescence*.

539

This is a **preprint**

The article has been submitted for peer-review to the *Journal of Luminescence* as:

Riedesel, S., Duller, G.A.T., Ankjærgaard, C., submitted. Time-resolved infrared stimulated luminescence of the blue and yellow-green emissions – insights into charge recombination in chemically and structurally different alkali feldspars. *Journal of Luminescence*.

540 **References**

- 541 Ankjærgaard, C., Jain, M., Kalchgruber, R., Lapp, T., Klein, D., McKeever, S.W.S., Murray, A.S.,
542 Morthekai, P., 2009. Further investigations into pulsed optically stimulated luminescence from
543 feldspars using blue and green light. *Radiation Measurements* 44, 576-581.
- 544 Ankjærgaard, C., Jain, M., 2010. Optically stimulated phosphorescence in orthoclase feldspar over the
545 millisecond to second timescale. *Journal of Luminescence* 130, 2346–2355.
- 546 Bailiff, I.K., 2000. Characteristics of time-resolved luminescence in quartz. *Radiation Measurements* 32,
547 401-405.
- 548 Bates, D. M. and DebRoy, S., 2018. nls function—nonlinear least squares R Core Team and contributors
549 worldwide, 2018. The R stats package version 3.5.0 (2018)
- 550 Chithambo, M.L., 2002. Time-resolved luminescence from annealed quartz. *Radiation Protection*
551 *Dosimetry* 100, 273-276.
- 552 Chithambo, M.L., 2003. Dependence of the thermal influence on luminescence lifetimes from quartz
553 on the duration of optical stimulation. *Radiation Measurements* 37, 167-175.
- 554 Chithambo, M.L., 2007. The analysis of time-resolved optically stimulated luminescence: II. Computer
555 simulations and experimental results. *Journal of Physics D: Applied Physics* 40, 1880-1889.
- 556 Clark, R.J., Bailiff, I.K., Tooley, M.J., 1997. A preliminary study of time-resolved luminescence in some
557 feldspars. *Radiation Measurements* 27, 211-220.
- 558 Clark, R.J., Bailiff, I.K., 1998. Fast time-resolved luminescence emission spectroscopy in some feldspars.
559 *Radiation Measurements* 29, 553-560.
- 560 Finch, A.A., Klein, J., 1999. The cause and petrological significance of cathodoluminescence emissions
561 from alkali feldspars. *Contributions to Mineralogy and Petrology* 135, 234-243.
- 562 Geake, J.E., Walker, G., Mills, A.A., Garlick, G.F.J., 1971. Luminescence of Apollo lunar samples.
563 *Proceedings of the Second Lunar Science Conference* 3, 2265-2275.
- 564 Geake, J.E., Walker, G., Telfer, D.J., Mills, A.A., Garlick, G.F.J., 1973. Luminescence of lunar, terrestrial,
565 and synthesized plagioclase caused by Mn²⁺ and Fe³⁺. *Proceedings of the Fourth Lunar Science*
566 *Conference* 4, 3181-3189.

This is a **preprint**

The article has been submitted for peer-review to the *Journal of Luminescence* as:

Riedesel, S., Duller, G.A.T., Ankjærgaard, C., submitted. Time-resolved infrared stimulated luminescence of the blue and yellow-green emissions – insights into charge recombination in chemically and structurally different alkali feldspars. *Journal of Luminescence*.

- 567 Geake, J.E., Walker, G., Telfer, D.J., Mills, A.A., 1977. The cause and significance of luminescence in
568 lunar plagioclase. *Philosophical transactions of the Royal Society A* 285, 403-408.
- 569 Jain, M., Ankjærgaard, C., 2011. Towards a non-fading signal in feldspar: Insight into charge transport
570 and tunnelling from time-resolved optically stimulated luminescence. *Radiation Measurements* 46,
571 292-309.
- 572 Jain, M., Guralnik, B., Andersen, M.T., 2012. Stimulated luminescence emission from localized
573 recombination in randomly distributed defects. *Journal of Physics: Condensed Matter* 24, 385402.
- 574 Kirsh, Y., Shoval, S., Townsend, P.D., 1987. Kinetics and emission spectra of thermoluminescence in the
575 feldspars albite and microcline. *Physica Status Solidi* 101, 253-262.
- 576 Kumar, R., Kook, M., Murray, A.S., Jain, M., 2018. Towards direct measurement of electrons in
577 metastable states in K-feldspar: Do infrared-photoluminescence and radioluminescence probe the
578 same trap? *Radiation Measurements* 120, 7-13.
- 579 Lapp, T., Jain, M., Ankjærgaard, C., Pritzel, L., 2009. Development of pulsed stimulation and Photon
580 Timer attachment to the Risø TL/OSL reader. *Radiation Measurements* 44, 571-575.
- 581 Lapp, T., Kook, M., Murray, A.S., Thomsen, K.J., Buylaert, J.P. and Jain, M., 2015. A new luminescence
582 detection and stimulation head for the Risø TL/OSL reader. *Radiation Measurements* 81, 178-184.
- 583 Pagonis, V., Morthekai, P., Singhvi, A.K., Thomas, J., Balaram, V., Kitis, G., Chen, R., 2012. Time-resolved
584 infrared stimulated luminescence signals in feldspars: Analysis based on exponential and stretched
585 exponential functions. *Journal of Luminescence* 132, 2330-2340.
- 586 Pagonis, V., Ankjærgaard, C., Jain, M., Chithambo, M.L., 2016. Quantitative analysis of time-resolved
587 infrared stimulated luminescence in feldspars. *Physica B* 497, 78-85.
- 588 Prasad, A.K., Lapp, T., Kook, M., Jain, M., 2016. Probing luminescence centres in Na rich feldspar.
589 *Radiation Measurements* 90, 292-297.
- 590 Rendell, H.M., Clarke, M.L., 1997. Thermoluminescence, radioluminescence and cathodoluminescence
591 spectra of alkali feldspars. *Radiation Measurements* 27, 263-272.
- 592 Riedesel, S., King, G.E., Prasad, A.K., Kumar, R., Finch, A.A., Jain, M., 2019. Optical determination of the
593 width of the band-tail states, and the excited and ground state energies of the principal dosimetric
594 trap in feldspar. *Radiation Measurements* 125, 40-51.

This is a **preprint**

The article has been submitted for peer-review to the *Journal of Luminescence* as:

Riedesel, S., Duller, G.A.T., Ankjærgaard, C., submitted. Time-resolved infrared stimulated luminescence of the blue and yellow-green emissions – insights into charge recombination in chemically and structurally different alkali feldspars. *Journal of Luminescence*.

- 595 Riedesel, S., Bell, A.M.T., Duller, G.A.T., Finch, A.A., Jain, M., King, G.E., Pearce, N.J., Roberts, H.M.,
596 2021a. Exploring sources of variation in thermoluminescence emissions and anomalous fading in alkali
597 feldspars. *Radiation Measurements* 141, 106541.
- 598 Riedesel, S., Kumar, R., Duller, G.A.T., Roberts, H.M., Bell, A.M.T., Jain, M., 2021b. Site-selective
599 characterisation of electron trapping centres in relation to chemistry, structural state and mineral
600 phases present in single crystal alkali feldspars. *Journal of Physics D: Applied Physics* 54, 385107.
- 601 Sanderson, D.C.W., Clark, R.J., 1994. Pulsed photostimulated luminescence of alkali feldspars.
602 *Radiation Measurements* 23, 633-639.
- 603 Telfer, D.J., Walker, G., 1978. Ligand field bands of Mn²⁺ and Fe³⁺ luminescence centres and their site
604 occupancy in plagioclase feldspars. *Modern Geology* 6, 199-210.
- 605 Thomsen, K.J., Murray, A.S., Jain, M., Bøtter-Jensen, L., 2008. Laboratory fading rates of various
606 luminescence signals from feldspar-rich sediment extract. *Radiation Measurements* 43, 1474-1486.
- 607 Tsukamoto, S., Denby, P.M., Murray, A.S., Bøtter-Jensen, L., 2006. Time-resolved luminescence from
608 feldspars: New insights into fading. *Radiation Measurements* 41, 790-795.
- 609 Tsukamoto, S., Murray, A.S., Ankjærgaard, C., Jain, M., Lapp, T., 2010. Charge recombination processes
610 in minerals studied using optically stimulated luminescence and time-resolved exo-electrons. *Journal*
611 *of Physics D: Applied Physics* 43, 325502.
- 612

This is a **preprint**

The article has been submitted for peer-review to the *Journal of Luminescence* as:

Riedesel, S., Duller, G.A.T., Ankjærgaard, C., submitted. Time-resolved infrared stimulated luminescence of the blue and yellow-green emissions – insights into charge recombination in chemically and structurally different alkali feldspars. *Journal of Luminescence*.

613

Supplementary Material

614

Time-resolved infrared stimulated luminescence of the blue and yellow-green emissions –

615

insights into charge recombination in chemically and structurally different alkali feldspars

616

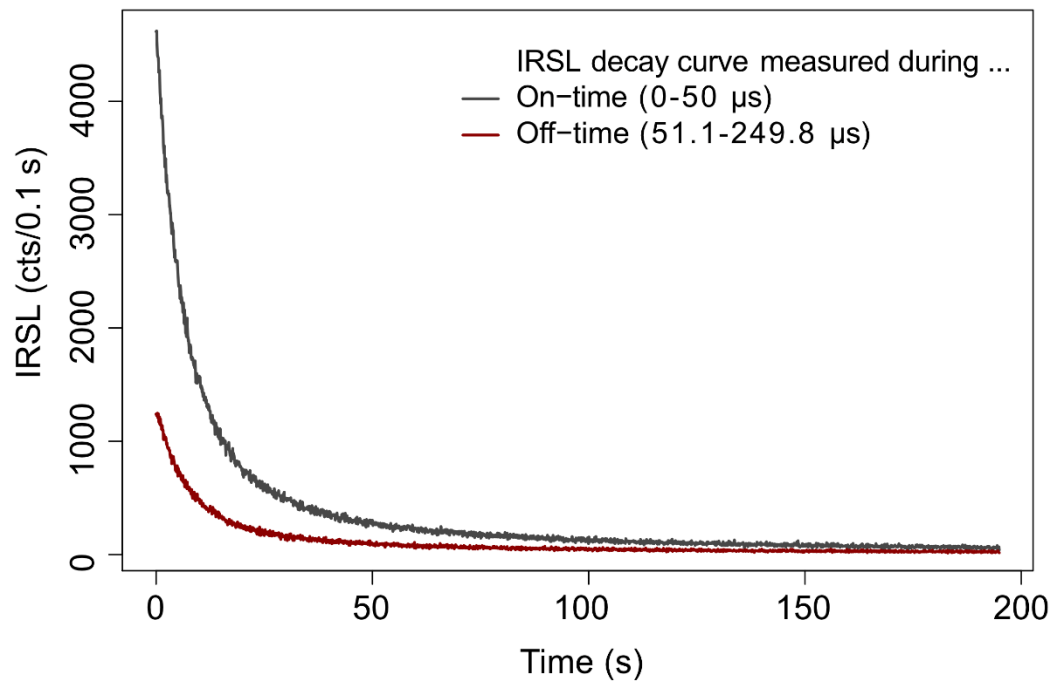


Fig. S1: IRSL₅₀ decay curves measured during the on- (0-50 μs, grey curve) and off-times (51.1-249.8 μs, red curve) of the TR-luminescence measurements recorded in the blue emission window.

617

618

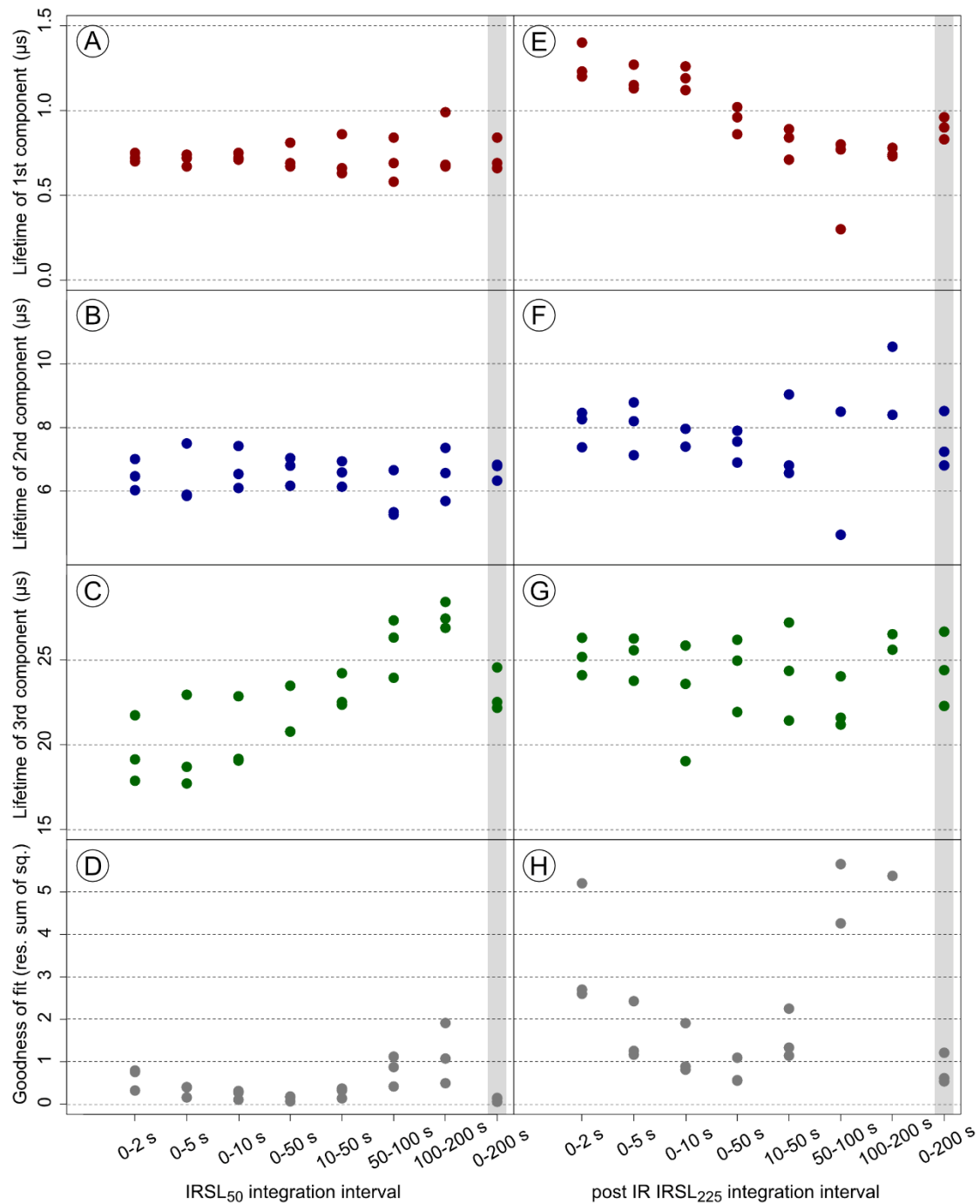


Fig. S2. Lifetimes and goodness of fit defined by the square sum of residuals for different integration time intervals for sample FSM-3. The data shown here is for the off-time signal of the blue emission and the two signals measured using the post-IR₅₀ IRSL₂₂₅ protocol, with results for the IRSL₅₀ signal in the left panels (A-D) and for the post-IR IRSL₂₂₅ on the right (E-H). The individual points show results for three aliquots measured.

619

620

This is a **preprint**

The article has been submitted for peer-review to the *Journal of Luminescence* as:

Riedesel, S., Duller, G.A.T., Ankjærgaard, C., submitted. Time-resolved infrared stimulated luminescence of the blue and yellow-green emissions – insights into charge recombination in chemically and structurally different alkali feldspars. *Journal of Luminescence*.

Table S1a: Lifetimes for the blue IRSL₅₀ emission recorded in the on-time of the pulsed IRSL signal. I_i is the normalised intensity of the fitted lifetime τ_i (μ s), k is a constant linear background. All values displayed are the average of three aliquots and the standard deviation. The data was normalised to the last data point of the on-time.

Sample ID	Dose (Gy)	I_1	τ_1	I_2	τ_2	I_3	τ_3	I_4	τ_4	k	residual sum of squares
FSM-13	50			1.00 ± 0.05	9.99 ± 0.27					0.01 ± 0.01	2.43 ± 0.72
FSM-13LH	50					1.56 ± 0.04	54.38 ± 0.76			0.04 ± 0.00	0.29 ± 0.07
FSM-3	50	0.61 ± 0.09	1.18 ± 0.18	0.42 ± 0.08	11.67 ± 0.22					-0.03 ± 0.01	0.50 ± 0.21
FSM-5	50	0.96 ± 0.05	1.13 ± 0.01	0.18 ± 0.03	12.79 ± 0.94					-0.10 ± 0.00	1.38 ± 0.47
FSM-6	50	0.29 ± 0.00	2.29 ± 0.19	0.76 ± 0.09	12.26 ± 3.09	0.25 ^a	79.39 ^a			0.00 ± 0.00	1.42 ± 0.90
FSM-6LH	50					1.33 ± 0.03	39.66 ± 2.33			0.05 ± 0.00	0.06 ± 0.02
CLBR	50	0.88 ± 0.05	4.21 ± 0.54			0.18 ± 0.09	23.19 ± 4.80			0.01 ± 0.06	0.42 ± 0.18
FSM-13	200			0.92 ± 0.05	9.49 ± 0.24					0.02 ± 0.00	3.75 ± 0.99
FSM-13LH	200					1.60 ± 0.05	53.26 ± 1.00			0.04 ± 0.00	0.55 ± 0.18
FSM-3	200	0.60 ± 0.09	1.18 ± 0.18	0.43 ± 0.07	11.81 ± 0.10					-0.02 ± 0.01	1.21 ± 0.36
FSM-5	200	0.76 ± 0.06	1.22 ± 0.04	0.26 ± 0.02	12.09 ± 0.77					-0.08 ± 0.01	3.00 ± 0.98
FSM-6	200	0.57 ± 0.19	5.58 ± 2.15	0.53 ± 0.19	20.19 ± 3.00					0.01 ± 0.02	3.72 ± 2.81
FSM-6LH	200					1.39 ± 0.03	42.34 ± 1.46			0.05 ± 0.00	0.44 ± 0.37
CLBR	200	0.91 ± 0.08	3.97 ± 0.19			0.17 ± 0.07	26.96 ± 5.78			-0.03 ± 0.01	1.15 ± 0.56
FSM-13	800			1.01 ± 0.05	9.77 ± 0.27					0.01 ± 0.01	6.46 ± 2.67
FSM-13LH	800			<i>Not measured due to very high signal intensities saturating the PMT despite adding an ND 2.0 filter.</i>							
FSM-3	800	0.54 ± 0.04	1.28 ± 0.46	0.50 ± 0.06	11.93 ± 1.29					0.00 ± 0.01	3.40 ± 1.37
FSM-5	800	0.70 ± 0.04	1.27 ± 0.06	0.36 ± 0.02	11.33 ± 0.75					-0.06 ± 0.01	1.73 ± 0.49
FSM-6	800			0.57 ± 0.29	6.08 ± 2.34	0.48 ± 0.24	27.76 ± 13.17			0.00 ± 0.03	1.17 ± 0.84
FSM-6LH	800			<i>Not measured due to very high signal intensities saturating the PMT despite adding an ND 2.0 filter.</i>							
CLBR	800	0.87 ± 0.12	3.99 ± 0.19			0.17 ± 0.07	32.27 ± 4.65			-0.03 ± 0.01	3.34 ± 1.54

This is a **preprint**

The article has been submitted for peer-review to the *Journal of Luminescence* as:

Riedesel, S., Duller, G.A.T., Ankjærgaard, C., submitted. Time-resolved infrared stimulated luminescence of the blue and yellow-green emissions – insights into charge recombination in chemically and structurally different alkali feldspars. *Journal of Luminescence*.

Table S1b: Lifetimes for the **blue IRSL₅₀** emission recorded in the **off-time** of the pulsed IRSL signal. I_i is the normalised intensity of the fitted lifetime τ_i (μ s), k is a constant linear background. All values displayed are the average of three aliquots and the standard deviation. The data was normalised to the last data point of the on-time.

Sample ID	Dose (Gy)	I_1	τ_1	I_2	τ_2	I_3	τ_3	I_4	τ_4	k	residual sum of squares
FSM-13	50			0.43 ± 0.13	5.25 ± 0.59	0.47 ± 0.14	13.27 ± 2.58	0.12 ± 0.02	39.99 ± 6.65	0.01 ± 0.00	0.88 ± 0.28
FSM-13LH	50							0.96 ± 0.02	45.08 ± 0.27	0.06 ± 0.00	0.63 ± 0.13
FSM-3	50	0.53 ± 0.08	0.73 ± 0.09	0.31 ± 0.05	6.65 ± 0.28			0.18 ± 0.04	23.08 ± 1.29	0.01 ± 0.00	0.11 ± 0.05
FSM-5	50	0.89 ± 0.04	0.83 ± 0.03	0.14 ± 0.02	7.52 ± 1.03			0.08 ± 0.01	24.39 ± 5.40	0.00 ± 0.00	0.16 ± 0.04
FSM-6	50			0.57 ± 0.10	6.64 ± 0.99			0.33 ± 0.05	24.24 ± 3.49	0.01 ± 0.00	0.58 ± 0.49
FSM-6LH	50							0.96 ± 0.01	43.08 ± 0.76	0.05 ± 0.00	0.21 ± 0.03
CLBR	50			0.78 ± 0.05	3.74 ± 0.26	0.16 ± 0.03	14.65 ± 2.13	0.03 ± 0.03	102.18 ± 64.17	0.06 ± 0.00	0.17 ± 0.08
FSM-13	200			0.40 ± 0.18	4.58 ± 1.63	0.45 ± 0.13	12.94 ± 3.26	0.11 ± 0.06	40.38 ± 8.46	0.001 ± 0.00	1.33 ± 0.45
FSM-13LH	200							0.99 ± 0.03	44.40 ± 0.38	0.06 ± 0.00	1.12 ± 0.39
FSM-3	200	0.51 ± 0.10	0.67 ± 0.13	0.32 ± 0.05	5.84 ± 0.61			0.20 ± 0.03	22.16 ± 0.86	0.01 ± 0.00	0.27 ± 0.09
FSM-5	200	0.71 ± 0.05	0.81 ± 0.08	0.21 ± 0.02	6.92 ± 1.05			0.10 ± 0.02	23.33 ± 2.93	0.00 ± 0.00	0.38 ± 0.12
FSM-6	200			0.63 ± 0.11	6.50 ± 1.07			0.38 ± 0.08	25.90 ± 5.09	0.02 ± 0.01	1.66 ± 1.48
FSM-6LH	200							0.96 ± 0.00	41.71 ± 0.18	0.05 ± 0.00	0.64 ± 0.65
CLBR	200			0.82 ± 0.04	3.58 ± 0.06	0.18 ± 0.01	15.55 ± 1.79	0.03 ± 0.02	87.11 ± 31.14	0.03 ± 0.00	0.40 ± 0.24
FSM-13	800			0.51 ± 0.18	5.38 ± 1.20	0.47 ± 0.11	14.92 ± 2.69	0.06 ± 0.04	53.26 ± 15.37	0.01 ± 0.00	2.46 ± 1.32
FSM-13LH	800			<i>Not measured due to very high signal intensities saturating the PMT despite adding an ND 2.0 filter.</i>							
FSM-3	800	0.45 ± 0.04	0.74 ± 0.26	0.36 ± 0.09	6.31 ± 1.64			0.21 ± 0.03	23.01 ± 3.36	0.01 ± 0.00	0.76 ± 0.36
FSM-5	800	0.64 ± 0.06	0.86 ± 0.03	0.29 ± 0.02	6.96 ± 0.34			0.12 ± 0.01	24.06 ± 2.65	0.01 ± 0.00	0.27 ± 0.06
FSM-6	800			0.59 ± 0.15	6.78 ± 1.32			0.37 ± 0.10	24.78 ± 4.03	0.01 ± 0.01	0.55 ± 0.47
FSM-6LH	800			<i>Not measured due to very high signal intensities saturating the PMT despite adding an ND 2.0 filter.</i>							
CLBR	800			0.76 ± 0.09	3.49 ± 0.18	0.18 ± 0.02	13.91 ± 1.38	0.04 ± 0.04	68.07 ± 37.48	0.03 ± 0.00	1.15 ± 0.73

This is a **preprint**

The article has been submitted for peer-review to the *Journal of Luminescence* as:

Riedesel, S., Duller, G.A.T., Ankjærgaard, C., submitted. Time-resolved infrared stimulated luminescence of the blue and yellow-green emissions – insights into charge recombination in chemically and structurally different alkali feldspars. *Journal of Luminescence*.

Table S2a: Lifetimes for the blue post-IR IRSL₂₂₅ emission recorded in the on-time of the pulsed IRSL signal. I_i is the normalised intensity of the fitted lifetime τ_i (μ s), k is a constant linear background. All values displayed are the average of three aliquots and the standard deviation. The data was normalised to the last data point of the on-time.

Sample ID	Dose (Gy)	I_1	τ_1	I_2	τ_2	I_3	τ_3	I_4	τ_4	k	residual sum of squares
FSM-13	50	0.53 ± 0.04	4.66 ± 0.07	0.48 ± 0.07	21.25 ± 3.95					0.03 ± 0.02	2.08 ± 0.87
FSM-13LH	50					1.28 ± 0.02	57.05 ± 1.16			0.26 ± 0.01	0.10 ± 0.02
FSM-3	50	0.71 ± 0.07	1.25 ± 0.10	0.19 ± 0.01	16.00 ± 1.58					0.13 ± 0.07	0.96 ± 0.42
FSM-5	50	0.80 ± 0.06	1.18 ± 0.02	0.29 ± 0.04	10.92 ± 3.50					-0.09 ± 0.01	1.01 ± 0.56
FSM-6	50			0.95 ± 0.04	10.94 ± 1.56					0.05 ± 0.03	0.70 ± 0.37
FSM-6LH	50					1.16 ± 0.04	32.53 ± 2.63			0.09 ± 0.01	0.04 ± 0.02
CLBR	50	0.81 ± 0.20	4.40 ± 0.37			0.31 ± 0.26	34.18 ± 17.84			0.04 ± 0.06	0.44 ± 0.23
FSM-13	200	0.60 ± 0.03	4.93 ± 0.67			0.39 ± 0.07	24.92 ± 5.48			0.01 ± 0.01	4.34 ± 0.14
FSM-13LH	200					1.24 ± 0.05	52.93 ± 1.67			0.25 ± 0.00	0.17 ± 0.04
FSM-3	200	0.63 ± 0.05	1.20 ± 0.08	0.17 ± 0.01	14.48 ± 0.06					0.17 ± 0.08	2.25 ± 0.82
FSM-5	200	0.80 ± 0.04	1.21 ± 0.08	0.25 ± 0.01	8.16 ± 1.29					-0.07 ± 0.01	2.34 ± 0.73
FSM-6	200			0.93 ± 0.07	10.61 ± 1.28					0.04 ± 0.03	1.23 ± 0.70
FSM-6LH	200					1.21 ± 0.03	35.87 ± 1.39			0.09 ± 0.00	0.28 ± 0.22
CLBR	200	0.80 ± 0.16	4.14 ± 0.24			0.24 ± 0.25 ^b	29.73 ± 6.83 ^b			0.06 ± 0.01	1.64 ± 0.72
FSM-13	800	0.57 ± 0.06	4.63 ± 0.41	0.45 ± 0.03	16.77 ± 2.37					0.00 ± 0.01	7.14 ± 3.32
FSM-13LH	800			<i>Not measured due to very high signal intensities saturating the PMT despite adding an ND 2.0 filter.</i>							
FSM-3	800	0.56 ± 0.14	1.26 ± 0.22	0.16 ± 0.01	14.39 ± 1.78					0.26 ± 0.12	6.52 ± 2.69
FSM-5	800	0.77 ± 0.02	1.23 ± 0.04	0.32 ± 0.02	8.25 ± 1.38					-0.06 ± 0.01	1.59 ± 0.48
FSM-6	800			0.97 ± 0.02	10.06 ± 0.88					0.03 ± 0.02	0.44 ± 0.29
FSM-6LH	800			<i>Not measured due to very high signal intensities saturating the PMT despite adding an ND 2.0 filter.</i>							
CLBR	800	0.79 ± 0.21	3.95 ± 0.38			0.45 ^a	25.64 ^a			0.06 ± 0.00	5.26 ± 2.42

This is a **preprint**

The article has been submitted for peer-review to the *Journal of Luminescence* as:

Riedesel, S., Duller, G.A.T., Ankjærgaard, C., submitted. Time-resolved infrared stimulated luminescence of the blue and yellow-green emissions – insights into charge recombination in chemically and structurally different alkali feldspars. *Journal of Luminescence*.

Table S2b: Lifetimes for the **blue post-IR IRSL₂₂₅** emission recorded in the **off-time** of the pulsed IRSL signal. I_i is the normalised intensity of the fitted lifetime τ_i (μ s), k is a constant linear background. All values displayed are the average of three aliquots and the standard deviation. The data was normalised to the last data point of the on-time.

Sample ID	Dose (Gy)	I_1	τ_1	I_2	τ_2	I_3	τ_3	I_4	τ_4	k	residual sum of squares
FSM-13	50			0.45 ± 0.07	4.13 ± 0.27	0.35 ± 0.05	14.31 ± 2.46	0.12 ± 0.02	39.99 ± 6.65	0.01 ± 0.00	0.88 ± 0.28
FSM-13LH	50							0.96 ± 0.02	45.08 ± 0.27	0.06 ± 0.00	0.63 ± 0.13
FSM-3	50	0.65 ± 0.07	0.89 ± 0.07	0.14 ± 0.02	7.52 ± 0.89			0.18 ± 0.04	23.08 ± 1.29	0.01 ± 0.00	0.11 ± 0.05
FSM-5	50	0.75 ± 0.05	0.90 ± 0.03	0.27 ± 0.03	8.82 ± 2.09			0.08 ± 0.01	24.39 ± 5.40	0.00 ± 0.00	0.16 ± 0.04
FSM-6	50			0.77 ± 0.12	8.95 ± 0.27			0.33 ± 0.05	24.24 ± 3.49	0.01 ± 0.00	0.58 ± 0.49
FSM-6LH	50							0.96 ± 0.01	43.08 ± 0.76	0.05 ± 0.00	0.12 ± 0.03
CLBR	50			0.73 ± 0.20	3.96 ± 0.32	0.12 ± 0.06	20.81 ± 7.25	0.03 ± 0.03	102.18 ± 64.17	0.06 ± 0.05	0.31 ± 0.29
FSM-13	200			0.45 ± 0.13	3.81 ± 0.80	0.37 ± 0.09	14.33 ± 4.51	0.11 ± 0.07	62.84 ± 39.90	0.05 ± 0.01	1.96 ± 0.73
FSM-13LH	200							0.77 ± 0.02	44.37 ± 0.04	0.27 ± 0.00	0.46 ± 0.12
FSM-3	200	0.57 ± 0.06	0.84 ± 0.11	0.13 ± 0.01	6.62 ± 1.48			0.08 ± 0.02	33.25 ± 1.37	0.22 ± 0.07	2.45 ± 1.24
FSM-5	200	0.73 ± 0.02	0.84 ± 0.03	0.28 ± 0.02	5.90 ± 0.76			0.03 ± 0.01	33.28 ± 2.88	0.01 ± 0.00	0.31 ± 0.09
FSM-6	200			0.77 ± 0.13	8.81 ± 0.19			0.16 ± 0.07	32.15 ± 4.08	0.07 ± 0.01	0.89 ± 0.67
FSM-6LH	200							0.90 ± 0.00	37.86 ± 0.31	0.10 ± 0.00	0.47 ± 0.37
CLBR	200			0.72 ± 0.15	3.71 ± 0.11	0.11 ± 0.04	14.05 ± 1.67	0.08 ± 0.12	94.63 ± 42.70	0.12 ± 0.02	1.25 ± 0.70
FSM-13	800			0.38 ± 0.10	3.41 ± 0.42	0.48 ± 0.06	10.96 ± 3.37	0.13 ± 0.08	37.63 ± 14.26	0.05 ± 0.00	3.51 ± 1.50
FSM-13LH	800			<i>Not measured due to very high signal intensities saturating the PMT despite adding an ND 2.0 filter.</i>							
FSM-3	800	0.52 ± 0.11	0.84 ± 0.20	0.15 ± 0.04	7.80 ± 1.80			0.06 ± 0.02	37.87 ± 4.60	0.29 ± 0.11	7.88 ± 3.03
FSM-5	800	0.69 ± 0.01	0.87 ± 0.04	0.32 ± 0.02	6.01 ± 0.58			0.05 ± 0.01	32.31 ± 3.06	0.02 ± 0.00	0.29 ± 0.07
FSM-6	800			0.85 ± 0.06	9.10 ± 0.17			0.11 ± 0.05	34.26 ± 3.42	0.07 ± 0.01	0.29 ± 0.24
FSM-6LH	800			<i>Not measured due to very high signal intensities saturating the PMT despite adding an ND 2.0 filter.</i>							
CLBR	800			0.70 ± 0.15	3.52 ± 0.32	0.10 ± 0.04	11.18 ± 1.97	0.10 ± 0.14	133.61 ± 111.59	0.12 ± 0.00	4.33 ± 3.14

This is a **preprint**

The article has been submitted for peer-review to the *Journal of Luminescence* as:

Riedesel, S., Duller, G.A.T., Ankjærgaard, C., submitted. Time-resolved infrared stimulated luminescence of the blue and yellow-green emissions – insights into charge recombination in chemically and structurally different alkali feldspars. *Journal of Luminescence*.

*Table S3a: Lifetimes for the **yellow-green IRSL₅₀** emission recorded in the **on-time** of the pulsed IRSL signal. I_i is the normalised intensity of the fitted lifetime τ_i (ms), k is a constant linear background. All values displayed are the average of three aliquots and the standard deviation. The data was normalised to the last data point of the on-time.*

Sample ID	Dose (Gy)	I_1	τ_1	I_2	τ_2	I_3	τ_3	I_4	τ_4	k	residual sum of squares
FSM-13	200	0.20 ± 0.01	0.22 ± 0.08	0.83 ± 0.02	2.50 ± 0.34					0.09 ± 0.01	0.06 ± 0.03
FSM-13LH	200	0.64 ± 0.06	0.05 ± 0.00	0.12 ± 0.05	2.52 ± 0.43					0.26 ± 0.00	0.01 ± 0.01
FSM-3	200	0.09 ± 0.03	0.02 ± 0.01			1.87 ± 0.18	8.52 ± 0.61			0.18 ± 0.02	0.04 ± 0.01
FSM-5	400	0.39 ± 0.01	0.02 ± 0.00	0.14 ± 0.00	3.93 ± 0.72					0.51 ± 0.01	0.27 ± 0.14
FSM-6	400	0.43 ± 0.14	0.04 ± 0.00	0.38 ± 0.49	4.04 ± 1.46					0.36 ± 0.11	0.05 ± 0.04
FSM-6LH	200	0.66 ± 0.01	0.04 ± 0.00	0.07 ± 0.00	2.13 ± 0.28					0.28 ± 0.00	0.01 ± 0.00
CLBR	200	0.10 ^a	0.03 ^a			2.43 ± 0.21	11.12 ± 1.55			0.13 ± 0.01	0.05 ± 0.05
FSM-13	800	0.20 ± 0.00	0.20 ± 0.04	0.82 ± 0.03	2.37 ± 0.19					0.09 ± 0.01	0.01 ± 0.01
FSM-13LH	800	0.66 ± 0.02	0.05 ± 0.00	0.08 ± 0.00	1.81 ± 0.08					0.27 ± 0.00	0.02 ± 0.01
FSM-3	800	0.11 ± 0.02	0.03 ± 0.01			1.57 ± 0.20	8.10 ± 0.67			0.20 ± 0.03	0.02 ± 0.01
FSM-5	800	0.38 ± 0.04	0.04 ± 0.00	0.15 ± 0.06	4.10 ± 2.38					0.53 ± 0.01	0.19 ± 0.06
FSM-6	800	0.37 ± 0.12	0.04 ± 0.00	0.65 ± 0.47	6.16 ± 1.76					0.31 ± 0.09	0.09 ± 0.06
FSM-6LH	800	0.64 ± 0.01	0.05 ± 0.00	0.08 ± 0.00	1.82 ± 0.41					0.27 ± 0.00	0.02 ± 0.01
CLBR	800	0.06 ^a	0.04 ^a			2.22 ± 0.10	9.66 ± 0.17			0.12 ± 0.01	0.01 ± 0.01

This is a **preprint**

The article has been submitted for peer-review to the *Journal of Luminescence* as:

Riedesel, S., Duller, G.A.T., Ankjærgaard, C., submitted. Time-resolved infrared stimulated luminescence of the blue and yellow-green emissions – insights into charge recombination in chemically and structurally different alkali feldspars. *Journal of Luminescence*.

*Table S3b: Lifetimes for the **yellow-green IRSL₅₀** emission recorded in the **off-time** of the pulsed IRSL signal. I_i is the normalised intensity of the fitted lifetime τ_i (ms), k is a constant linear background. All values displayed are the average of three aliquots and the standard deviation. The data was normalised to the last data point of the on-time.*

Sample ID	Dose (Gy)	I_1	τ_1	I_2	τ_2	I_3	τ_3	I_4	τ_4	k	residual sum of squares
FSM-13	200	0.19 ± 0.03	0.24 ± 0.06	0.57 ± 0.02	2.19 ± 0.17	0.14 ± 0.04	9.58 ± 1.12			0.01 ± 0.00	0.05 ± 0.02
FSM-13LH	200	0.52 ± 0.02	0.12 ± 0.01	0.07 ± 0.04	6.09 ± 0.39					0.03 ± 0.02	0.15 ± 0.04
FSM-3	200	0.13 ± 0.01	0.11 ± 0.01			0.75 ± 0.04	11.04 ± 0.06			0.03 ± 0.01	0.14 ± 0.08
FSM-5	400	0.40 ± 0.01	0.09 ± 0.00			0.08 ± 0.00	10.18 ± 0.70			0.06 ± 0.00	0.39 ± 0.04
FSM-6	400	0.37 ± 0.13	0.10 ± 0.00	0.08 ± 0.06	5.35 ± 2.24	0.15 ± 0.23	32.98 ± 21.06			0.03 ± 0.02	0.19 ± 0.00
FSM-6LH	200	0.52 ± 0.00	0.11 ± 0.00	0.04 ± 0.00	6.55 ± 0.06					0.01 ± 0.00	0.17 ± 0.18
CLBR	200			0.17 ± 0.05	3.90 ± 1.34	0.75 ± 0.03	13.53 ± 0.90			0.08 ± 0.01	0.21 ± XX
FSM-13	800	0.20 ± 0.01	0.24 ± 0.03	0.58 ± 0.01	2.13 ± 0.09	0.13 ± 0.02	8.56 ± 0.96			0.01 ± 0.00	0.02 ± 0.01
FSM-13LH	800	0.53 ± 0.01	0.11 ± 0.00	0.04 ± 0.00	6.52 ± 0.06					0.02 ± 0.00	0.18 ± 0.02
FSM-3	800	0.24 ± 0.16	0.10 ± 0.01			0.51 ± 0.37	10.55 ± 0.51			0.04 ± 0.00	0.15 ± 0.12
FSM-5	800	0.31 ± 0.16	0.10 ± 0.02			0.23 ± 0.25	9.59 ± 0.12			0.11 ± 0.11	0.23 ± 0.05
FSM-6	800	0.32 ± 0.12	0.10 ± 0.01	0.11 ± 0.04	4.23 ± 2.34	0.23 ± 0.18	19.80 ± 11.31			0.02 ± 0.02	0.21 ± 0.04
FSM-6LH	800	0.52 ± 0.01	0.11 ± 0.00	0.05 ± 0.00	6.33 ± 0.15					0.01 ± 0.00	0.17 ± 0.01
CLBR	800	0.04 ^a	0.14 ^a	0.24 ± 0.02	5.34 ± 0.29	0.69 ± 0.04	14.90 ± 0.31			0.07 ± 0.02	0.06 ± 0.05

This is a **preprint**

The article has been submitted for peer-review to the *Journal of Luminescence* as:

Riedesel, S., Duller, G.A.T., Ankjærgaard, C., submitted. Time-resolved infrared stimulated luminescence of the blue and yellow-green emissions – insights into charge recombination in chemically and structurally different alkali feldspars. *Journal of Luminescence*.

Table S4a: Lifetimes for the yellow-green post-IR IRSL₂₂₅ emission recorded in the on-time of the pulsed IRSL signal. I_i is the normalised intensity of the fitted lifetime τ_i (ms), k is a constant linear background. All values displayed are the average of three aliquots and the standard deviation. The data was normalised to the last data point of the on-time. ^aOnly one aliquot of the three aliquots measured revealed this lifetime.

Sample ID	Dose (Gy)	I_1	τ_1	I_2	τ_2	I_3	τ_3	I_4	τ_4	k	residual sum of squares
FSM-13	200	0.32 ± 0.03	0.12 ± 0.04	0.52 ± 0.04	1.92 ± 0.41					0.21 ± 0.02	0.07 ± 0.04
FSM-13LH	200	0.57 ± 0.00	0.05 ± 0.00	0.19 ± 0.00	2.06 ± 0.03					0.26 ± 0.00	0.01 ± 0.00
FSM-3	200	0.08 ± 0.01	0.03 ± 0.01			1.18 ± 0.20	7.14 ± 0.81			0.33 ± 0.03	0.11 ± 0.03
FSM-5	400	0.37 ^a	0.02 ^a	0.11 ^a	2.80 ^a					0.54	0.22
FSM-6	400	0.38 ± 0.02	0.04 ± 0.01	0.16 ± 0.01	2.35 ± 0.52					0.49 ± 0.00	0.06 ± 0.03
FSM-6LH	200	0.59 ± 0.00	0.04 ± 0.00	0.09 ± 0.01	1.59 ± 0.15					0.32 ± 0.00	0.01 ± 0.00
CLBR	200	0.24 ^a	0.04 ^a			2.39 ± 0.72	15.48 ± 4.07			0.31 ± 0.08	0.06 ± 0.06
FSM-13	800	0.32 ± 0.02	0.11 ± 0.01	0.52 ± 0.03	1.73 ± 0.18					0.19 ± 0.01	0.02 ± 0.01
FSM-13LH	800	0.56 ± 0.00	0.05 ± 0.00	0.19 ± 0.01	2.07 ± 0.12					0.27 ± 0.00	0.01 ± 0.00
FSM-3	800	0.08 ± 0.02	0.07 ± 0.07			1.10 ± 0.08	6.96 ± 0.56			0.35 ± 0.04	0.06 ± 0.02
FSM-5	800	0.33 ± 0.10	0.05 ± 0.03	0.09 ± 0.04	1.99 ± 0.63					0.58 ± 0.07	0.28 ± 0.11
FSM-6	800	0.44 ± 0.05	0.03 ± 0.00	0.13 ± 0.06	1.91 ± 0.30					0.46 ± 0.03	0.05 ± 0.04
FSM-6LH	800	0.59 ± 0.02	0.04 ± 0.00	0.11 ± 0.01	1.41 ± 0.36					0.31 ± 0.00	0.02 ± 0.01
CLBR	800	0.19 ^a	0.05 ^a			2.07 ± 0.45	12.35 ± 2.25			0.27 ± 0.06	0.02 ± 0.02

This is a **preprint**

The article has been submitted for peer-review to the *Journal of Luminescence* as:

Riedesel, S., Duller, G.A.T., Ankjær, C., submitted. Time-resolved infrared stimulated luminescence of the blue and yellow-green emissions – insights into charge recombination in chemically and structurally different alkali feldspars. *Journal of Luminescence*.

Table S4b: Lifetimes for the **yellow-green post-IR IRSL₂₂₅** emission recorded in the **off-time** of the pulsed IRSL signal. I_i is the normalised intensity of the fitted lifetime τ_i (ms), k is a constant linear background. All values displayed are the average of three aliquots and the standard deviation. The data was normalised to the last data point of the on-time. ^aOnly one aliquot of the three aliquots measured revealed this lifetime.

Sample ID	Dose (Gy)	I_1	τ_1	I_2	τ_2	I_3	τ_3	I_4	τ_4	k	residual sum of squares
FSM-13	200	0.33 ± 0.05	0.18 ± 0.04	0.33 ± 0.04	1.58 ± 0.02	0.12 ± 0.05	10.13 ± 0.82			0.07 ± 0.01	0.09 ± 0.03
FSM-13LH	200	0.47 ± 0.00	0.12 ± 0.00	0.10 ± 0.00	2.81 ± 0.09	0.05 ± 0.00	16.35 ± 0.79			0.05 ± 0.00	0.11 ± 0.00
FSM-3	200	0.13 ± 0.01	0.12 ± 0.02			0.56 ± 0.04	9.54 ± 0.22			0.18 ± 0.03	0.44 ± 0.12
FSM-5	400	0.42 ± 0.02	0.09 ± 0.00			0.05 ± 0.00	9.64 ± 0.70			0.02 ± 0.00	0.31 ± 0.07
FSM-6	400	0.40 ± 0.02	0.09 ± 0.00	0.06 ± 0.01	2.46 ± 0.31	0.06 ± 0.01	12.67 ± 0.03			0.06 ± 0.01	0.16 ± 0.02
FSM-6LH	200	0.50 ± 0.00	0.11 ± 0.00	0.04 ± 0.00	3.57 ± 0.07	0.01 ± 0.00	28.54 ± 2.43			0.02 ± 0.00	0.16 ± 0.01
CLBR	200	0.22 ^a	0.14 ^a			0.57 ± 0.03	11.36 ± 0.18	0.21 ± 0.00 ^b	56.08 ± 17.86 ^b	0.19 ± 0.08	0.23 ± 0.11
FSM-13	800	0.32 ± 0.02	0.18 ± 0.01	0.36 ± 0.03	1.58 ± 0.13	0.10 ± 0.03	9.87 ± 1.10			0.07 ± 0.01	0.04 ± 0.01
FSM-13LH	800	0.46 ± 0.00	0.12 ± 0.00	0.10 ± 0.00	2.68 ± 0.04	0.05 ± 0.00	16.15 ± 0.32			0.05 ± 0.00	0.11 ± 0.00
FSM-3	800	0.14 ± 0.02	0.12 ± 0.01			0.60 ± 0.09	9.73 ± 0.99			0.14 ± 0.10	0.22 ± 0.13
FSM-5	800	0.40 ± 0.02	0.09 ± 0.00			0.07 ± 0.01	7.23 ± 0.30			0.02 ± 0.00	0.25 ± 0.03
FSM-6	800	0.41 ± 0.03	0.09 ± 0.00	0.05 ± 0.02	4.13 ± 3.30	0.05 ± 0.01	13.96 ± 1.24			0.06 ± 0.01	0.18 ± 0.02
FSM-6LH	800	0.50 ± 0.00	0.11 ± 0.00	0.05 ± 0.00	3.30 ± 0.16	0.02 ± 0.00	21.06 ± 2.90			0.03 ± 0.00	0.16 ± 0.00
CLBR	800	0.17 ^a	0.12 ^a			0.36 ± 0.20	8.30 ± 3.36	0.37 ± 0.11	22.71 ± 7.49	0.19 ± 0.08	0.10 ± 0.07

This is a **preprint**

The article has been submitted for peer-review to the *Journal of Luminescence* as:

Riedesel, S., Duller, G.A.T., Ankjærgaard, C., submitted. Time-resolved infrared stimulated luminescence of the blue and yellow-green emissions – insights into charge recombination in chemically and structurally different alkali feldspars. *Journal of Luminescence*.

1